https://doi.org/10.5194/essd-2020-71
Preprint. Discussion started: 7 September 2020

Open Access Earth System Science Data Discussions

Consolidating the Randolph Glacier Inventory and the Glacier Inventory of China over the Qinghai-Tibetan Plateau and Investigating Glacier Changes Since the mid-20th Century

Xiaowan Liu[1,2,3], Zongxue Xu[1,2], Hong Yang[3,4], Xiuping Li[5], Dingzhi Peng[1,2]
[1]College of Water Sciences, Beijing Normal University, Beijing, 100875, China
[2]Beijiing Key Laboratory of Urban Hydrological Cycle and Sponge City Technology, Beijing, 100875, China
[3]Eawag, Swiss Federal Institute of Aquatic Science and Technology, 8600 Dübendorf, Switzerland
[4]Department of Environmental Science, MGU University of Basel, Petersplatz 1, 4001, Switzerland
[5]Institute of Tibetan Plateau Research, Chinese Academy of Sciences, Beijing, 100101, China

Correspondence to: Zongxue Xu (zongxuexu@vip.sina.com)

Abstract. Glacier retreat in the Qinghai-Tibetan Plateau (QTP), the 'third pole of the world', has attracted the attention of researchers worldwide. Glacier inventories in the 1970s and the 2000s provide valuable information to infer changes in individual glaciers. However, individual glacier volumes are either missing, incomplete or have large errors in these inventories, and thus, the use of these datasets to investigate changes in glaciers in QTP in the past few decades has become a challenge, particularly in the context of climate change. In this study, individual glacier volume data in the Randolph Glacier Inventory version 4.0 (RGI 4.0, 1970s) and the second Glacier Inventory of China (GIC-II, 2000s) are recalculated and consolidated using a slope-dependent algorithm based on elevation datasets for the QTP. The two consolidated inventories (The data are available under https://doi.org/10.11888/Glacio.tpdc.270390 (Liu, 2020). For the time of review, the data will be accessible through the following review link https://data.tpdc.ac.cn/en/data/4b88e394-0eb4-44c4-aa38-32aeb614daff/.) are validated by comparing the observed and estimated glacier data reported in the literature. The two consolidated glacier inventories are then compared for different mountains over the QTP to detect changes in glacier areas, volumes, fragmentation status, etc. during the past 3-4 decades. Based on the results, the slope-dependent algorithm performed well in computing individual glacier volumes and other elements, compared with the widely used volume-area scaling which often leads to overestimation in the interior Plateau and underestimation in other areas of the QTP in both RGI 4.0 and GIC-II. The comparison of the two inventories reveals a total area of glaciers in the QTP of approximately 59026.5 km^2 in the RGI 4.0 and 44301.2 km^2 in the GIC-Ⅱ. The total glacier volume is 4045.9 km^3 in the GIC-Ⅱ compared with 4716.7 km^3 in the RGI 4.0. The results suggest a significant retreat and melting of glaciers in the QTP. However, variations are observed in different glaciers. The Karakoram Mountains contain the largest number of surged glaciers, while the highest level of retreat is observed in the Gandise Mountains. An increase in the fragmentation index is observed in the northern mountains, particularly the Pamir Plateau, which displays the highest trends of glacier movement and deformation. The glacier volumes decrease mainly on south-westward aspects and increase to various extents on the other aspects of most mountains. The consolidation of the glacier inventories and the findings of the analysis performed in this study provide important databases for future glacier-related studies, particularly for investigating the effects of climate change on glaciers in the past and projecting future effects.

Key words. ice volume; RGI 4.0; GIC-II; glacier retreat; Himalayan Mountains; Qinghai-Tibetan Plateau

https://doi.org/10.5194/essd-2020-71
Preprint. Discussion started: 7 September 2020

1 Introduction

1.1 Background

Glacier melting and retreat in the context of climate change have attracted increasing attention in the recent years. Changes in glacier volumes and areas have been the focus of many studies due to their significant effects on the hydrological cycle and feedback effects on climate circulation (Bolch, 2007; Zhu et al., 2018). The Qinghai-Tibetan Plateau (QTP) has the largest ice storage, with an ice volume only inferior to polar regions (Liu et al., 2000). Glaciers over the QTP are shrinking, particularly in recent decades, due to global warming (Kang et al., 2010). According to the study by Qiu (2008), over eighty percent of glaciers in the QTP has been retreating since the 1960s. A study led by a distinguished expert in glacier studies in China predicted that approximately two-thirds of the glaciers in the QTP would disappear in 2050s with the current retreating rate (Yao et al., 2012b). Glacier melting exerts substantial effects on river runoff. The most direct results include short-term flooding, long-term drought, and intensifying/aggravating glacier-dammed lake, and disrupting the ecological balance, among others (Benn et al., 2012; Kaushik et al., 2019; Li, 2012; Zhang et al., 2015). Moreover, as a link to the global water cycle and energy transport, glacier retreat in the QTP may also alter the global climate. Thus, an understanding of the changes in glaciers in the QTP is essential for both runoff and global change projections.

1.2 Literature review

Numerous efforts have been focused on glacier-related studies over the QTP in the past few decades. These studies cover a wide range of aspects, such as the development of glacier monitoring and mapping technology, glacier melt modelling, glacier mass balance calculations, the contribution of glacial meltwater to runoff, and the interrelations between glacier retreat and climate change (Che et al., 2018; Gao et al., 2018; Zhu et al., 2018). Many studies have focused on the ice mass balance in the future, causes of glacier retreat and effective adaptations. However, due to the late start of glacier studies in the QTP, many efforts are still at the stage of collecting basic data, such as the topographic and geomorphological information, as well as long-term field observations of ice thickness, length and storage change in individual locations. A scientific group in the Institute of Cold and Arid Regions Environmental and Engineering Research of the Chinese Academy of Sciences has conducted a series of experiments and confirmed that glaciers at the northward aspect of the Himalayan Mountains trace monsoon changes over a long historical period (Ma et al., 2010). Another important finding is that small glaciers tend to be thinner when they span a greater vertical range because a greater vertical range is associated with greater slopes, velocities, and driving stresses (Haeberli and Hoelzle, 1995).

Studies of the relationships between the thickness, area and volume of different glaciers are currently mainly based on empirical parameters. For instance, Erasov (1968) described the relationship between area (A) and volume (V) as $V=0.027\cdot A^{1.5}$ for glaciers in central Asia. The Lanzhou Institute of Glaciology and Geocryology in China (LIGG) (1986) defined the empirical relation between the glacier area and volume for the glaciers in western China as $V=H\cdot A/1000$, and $H=53.2\cdot A^{0.3}-11.3$ (where H is the ice thickness). This equation was created to estimate the glacier volume for a large region with numerous glaciers in China. Machereet et al. (1988) indicated the relationship between the area and volume of the glaciers in the Altai-Tien Mountains as $V=0.0298\cdot A^{1.379}$. Liu et al. (2003) proposed the equation $V=0.0395\cdot\cot(A^{1.35})$" for glaciers in the Qilian and Tien Mountains in Northwest China.

https://doi.org/10.5194/essd-2020-71
Preprint. Discussion started: 7 September 2020

However, the vertical extent of a glacier mostly spans a larger range of climatic conditions with a greater mass balance difference from top to bottom. As a result, the flow at the equilibrium line is greater, which dominates for larger glaciers (Grinsted, 2013). This point challenges the accuracy of volumes determined using the area-volume scaling law on which the equations presented above are based. Hence, more field measurements must be collected and new methods must be explored to obtain more accurate estimates of glacier volumes. With the development of technology, field altimetry technology, such as airborne radio-echo sounding tracks, has been widely used. For instance, one of the bedrock topography products was provided by CReSIS, University of Kansas and NASA Operation Ice Bridge (https://data.cresis.ku.edu/). The Greenland Ice Mapping Project (GIMP) also employed this technology and published the surface elevation measurement data (Howat et al., 2014). Subsequently, the Ice Thickness Models Intercomparison Experiment (Farinotti et al., 2017; ITMIX) assessed the ability of seventeen different approaches to reproduce the observed thickness for various glacier types around the globe. An outstanding approach among these techniques is the ground-penetrating radar (GPR), which is considered to possess a strong penetration function (Sun et al., 2002). GPR has been widely used to detect ice thickness (Wang and Pu, 2009; Wu et al., 2011), subglacial topography (Zhu et al., 2014), and glacial hydrology features in recent years. The combination of GIS, GPS and GPR provides access to knowledge of the ice thickness and volume distribution (Ma et al., 2010). In China, GPR has been implemented in many cold areas for glacier monitoring since the 1980s (Wang and Pu, 2009; Ma et al., 2010; Zhu et al., 2014; Huai et al., 2015).

1.3 Purpose of this study

Given the importance of the QTP in global water systems and climate systems, as well as the trend of glacier melting amid global warming, complete databases/inventories are needed to record the glacier status and changes over the years. The glacier volume data are essential for glacier-related studies, particularly for understanding the effects of climate change. However, the complicated topographic and geomorphological conditions, and harsh weather in the glacial area pose substantial challenges to the monitoring projects. The implementation of field monitoring would not only require efficient technologies, but also large labour and financial resources. The existing field observations are extremely scattered and very scarce. Therefore, a tool that compiles glacier inventories based on the available remote sensing products and an appropriate calculation algorithm are necessary. Currently, several glacier inventories have been complied. The Randolph Glacier Inventory (RGI, it has version 1.0, 2.0, 3.2, 4.0, 5.0 and 6.0), and the First and Second Glacier Inventory of China (written as GIC-I and GIC-II, respectively, below) are the most comprehensive inventories covering the QTP. The information contains the minimum, median and maximum elevations, central location, mean slope, aspect, and area for each glacier. Many aspects of data from glaciers in the Chinese territory included in the Randolph Glacier Inventory have been improved based on the GIC-I (but the original GIC-I inventory is not available online). Meanwhile, the RGI 4.0, 5.0 and 6.0 have been improved substantially compared to RGI 1.0, 2.0, and 3.0. In terms of the data source dates over the QTP, 84.34% of images were collected from 1956~1980 in RGI 4.0, while all source maps in the RGI 5.0 and RGI 6.0 were obtained from 1998~2010. GIC-Ⅱ includes the glacier data representing the situation since 2000.

Glacier outline maps in different periods are required to study glacier evolution under the changing climate conditions. The two inventories, RGI 4.0 and GIC-II, provide the opportunity to investigate the effects of climate change on glaciers in QTP in the past few decades. However, RGI 4.0 did not provide information on glacier

https://doi.org/10.5194/essd-2020-71
Preprint. Discussion started: 7 September 2020

volumes, while the data in GIC-II contain some overestimations/underestimations compared with the observed data. Meanwhile, the mean thickness of the glaciers is not provided in either inventory. These gaps must be filled and the existing data in the two inventories must be verified to provide robust databases for glacier-related studies.

This study has two aims. The first is to recover the individual glacier volumes over the QTP based on the existing glacier information in RGI 4.0 and GIC-Ⅱ. A slope-dependent algorithm (the specific description is provided in Section 4.1) is applied for the calculation. The recalculated glacier volumes will be validated with the data from published studies and field observations. The second aim is to investigate the effects of climate change impacts by comparing the two glacier inventories, which represent the statuses at different periods. The results can provide a basis for understanding the glacier evolution in the QTP in the context of climate change. Moreover, the comparison would be helpful to capture the association between glacial retreat or advance with different atmospheric circulation patterns, which will enable a re-tracking the signal of historical climate change and project the changes into the future.

2 Study area

2.1 Topographical and geomorphological characteristics

The QTP is located in western China and surrounded by a large number of huge mountains (Figure 1), including southern Himalayan, northern Qilian, Kunlun, western Karakorum, eastern Hengduan, and interior Tangula, Gandise, and Nyainqentanglha Mountains. The majority of mountains extend from northwest to southeast. Most have a height greater than 6000 m a.s.l. (above sea level), whereas the elevation at many mountain peaks in the Himalayas even exceeds 8000 m a.s.l. In general, the average elevation over the entire QTP with total area of approximately 2.5 million km^2 is greater than 4000 m a.s.l. Thus, the QTP has two nicknames: “the Third Pole” of the earth and “The Water Tower of Asia”.

The unique geomorphology of the QTP has largely resulted in the boundary discrepancy, with high mountains located at the southwestern border and deep cuts located at the eastern margin. Due to the block of high topography at southwestern border, water vapour from the Indian Summer Monsoon (the main source of water vapour) is largely prevented from reaching the interior of the QTP. Only the area at southeastern Plateau with a large water vapour channel intercepts a large amount of precipitation (the annual precipitation exceeds 4000 mm).

https://doi.org/10.5194/essd-2020-71
Preprint. Discussion started: 7 September 2020

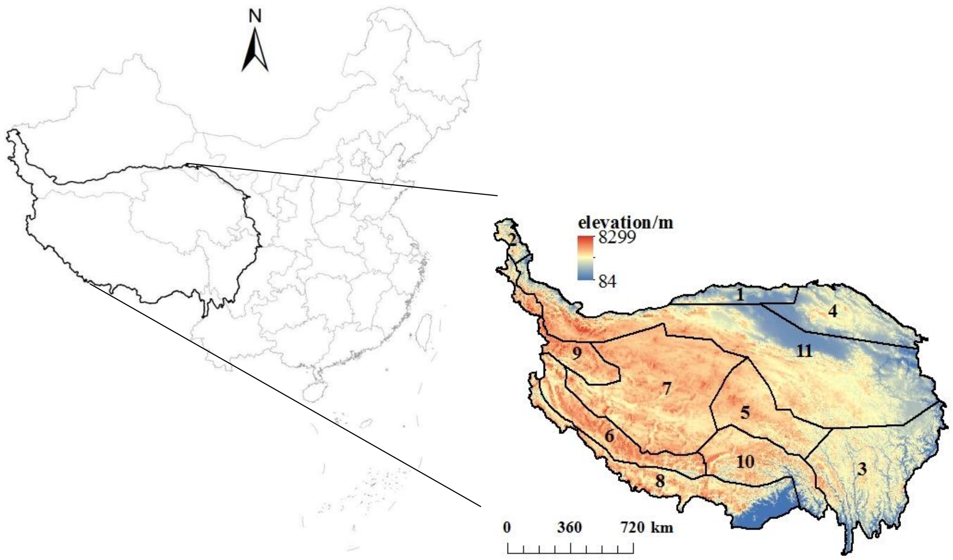

Fig. 1 Location and surface elevation pattern of the QTP in China

Note: 1-Altin Mountains (length: 730 km; width: 100 km); 2-Pamir Plateau (area: 10^5 km^2; length: 260 km; width: 50-100 km); 3-Hengduan Mountains (area: 6×10^5 km^2; length: 900 km); 4-Qilian Mountains (length: 800 km; width: 200-400 km); 5-Tangula Mountains (length: 700 km; width: 150 km); 6-Gandise Mountains (length: 1100 km; width: 60-100 km); 7-Qiangtang Plateau (area: 5.97×10^5 km^2; length: 1200 km; width: 760 km); 8-Himalayan Mountains (length: 2450 km; width: 200-350 km); 9-Karakoram Mountains (length: 800 km; width: 240 km); 10-Nyainqentanglha Mountains (length: 1400 km; width: 80 km); and 11-Kunlun Mountains (area: 5×10^5 km^2; length: 2500 km; width: 130-200 km) (Guo, 2011).

2.2 Glaciers and climate change

Glacier changes in the QTP are largely attributed to the changing regional water vapour and energy conditions (Deng and Zhang, 2018; Qiu, 2008). The sources of water vapour over this region mainly include the Indian Summer Monsoon, westerlies and East Asia Monsoon (Moor and Stoffel, 2013). In the context of global climate change, these climate systems are altered, causing changes in the glaciers located in the QTP. Due to its complicated topography and geomorphology, and monsoon-surrounded atmospheric circulation conditions, regional warming over the QTP is quite substantial and three times higher than other areas in China (Qiu, 2008; Yao et al., 2012a). The warming climate induces glacier melting.

The QTP has a typical plateau climate with low temperatures and strong solar radiation (Luo et al., 2004). The isotherm in the QTP is rising from the northeast and eastern borders to the southwestern area, with the lowest isotherm in the Qilian Mountains and the eastern margin of the plateau and the highest isotherm in the southwestern plateau (Yao and Zhang, 2015). The distribution of annual precipitation in the QTP shows a decreasing trend from southeastern to northwestern areas (Qi et al., 2013). In general, the climate in the QTP presents a pattern of warm-wet in the southeast and dry-cold in the northwest (Wang et al., 2002).

https://doi.org/10.5194/essd-2020-71
Preprint. Discussion started: 7 September 2020

3 Input Data

3.1 Randolph Glacier Inventory version 4.0 (RGI 4.0)

The Randolph Glacier Inventory 4.0 (RGI 4.0, http://www.glims.org/RGI/randolph40.html, doi:10.7265/N5-RGI-40)) (RGI Consortium, 2014) was released on 1 December 2014 by Global Land Ice Measurements from Space (GLIMS), which is a project designed to sketch glacier outlines all over the world based on the database obtained from optical satellite instruments (Raup et al., 2007). The RGI 4.0 includes the glacier information on central location, area, mean slope, mean aspect, maximum elevation, median elevation and minimum elevation for each glacier. The glaciers in the Chinese territory in the RGI 4.0 were compared to the first Glacier Inventory of China (GIC-I) based on topographic maps, aerial photographs and field measurements conducted in 1950s-1980s (Shi et al., 2008, 2009; Wu & Li, 2004). Some empirical observations reported in scientific publications were used to further validate the Chinese glacier data in the RGI 4.0, including the glacier inventory in the Nyainqentanglha Range of southeastern Tibet from Bolch et al. (2010), a glacier layer from the Digital Chart of the World (DCW) and the World Glacier Inventory (Raup et al., 2000; Haeberli et al., 1989; Haeberli et al., 1998). Most glacier outlines in the central and eastern Himalayas and Karakoram Mountains were obtained from the project of International Centre for Integrated Mountain Development (ICIMOD) (Bhambri et al., 2013; Frey et al., 2012; Mool et al., 2007; Raup et al., 2007), glacier outlines of the northeastern Karakoram Mountains were obtained from the study by Bhambri et al. (2013), and most data on the northern slopes of the Himalayas and the northeastern part of the Karakoram Mountains were obtained from the GIC-I (Shi et al., 2009).

3.2 The second Glacier Inventory of China (GIC-II)

The basic information for each glacier in the GIC-II (http://westdc.westgis.ac.cn, doi:10.3972/glacier.001.2013.db) (Guo et al., 2014) is same as the RGI 4.0. The GIC- II reported the above-mentioned glacier properties during 2007-2012 based on 218 Landsat images (http://earthexplorer.usgs.gov/), in which the widely-used band-ratio segmentation and manual adjustment were applied to outline glaciers. Meanwhile, several high-resolution images and Global Positioning System (GPS) measurements were combined to validate the results of glacier delineation. Delineations of the ice divide were based on DEMs (cell size of 30m) generated from digitized topographic maps, which were mainly constructed from aerial photographs acquired during the 1950s-1980s. In addition, two types of digital elevation models (DEMs) were used during the compilation of GIC-II to acquire altitudinal range of individual glaciers. A seven-coefficient transformation was employed on the elevation points and the digitized contours before DEM generation in order to minimize potential errors introduced by the mismatch in different coordinate systems, like Landsat images and topographic maps. The coefficients were obtained from coordinates of national trigonometric stations within and around maps collected from the Mapping and Geoinformation of China, the National Administration of Surveying. In the process, the Shuttle Radar Topographic Mission (SRTM) DEM from the Consultative Group for International Agriculture Research (CGIAR) version 4, where voids were filled using different auxiliary DEMs (http://srtm.csi.cgiar.org), were used to derive topographic attributes of the glaciers (Guo et al., 2014, 2015).

3.3 Bedrock elevation map and Digital Elevation Model outputs

ETOPO1 Global Relief Model was built using GMT 4.3.1 (http://gmt.soest.hawaii.edu/). GMT 4.3.1 creates grids with the spatial resolution of 1 arc-minute (625 m) in a netCDF COARDS-compliant format. The grid of the Earth's surface successfully depicts the bedrock underneath the ice sheets using ETOPO1 (https://www.ngdc.noaa.gov/mgg/global/global.html, doi:10.7289/V5C8276M) (Soller and Garrity, 2018). The bedrock elevation dataset was obtained by using the MB-System (http://www.ldeo.columbia.edu/res/pi/MB-System/) based on sixteen datasets, including Antarctica RAMP Topography, Antarctica BEDMAP Bedrock, Greenland NSIDC Bedrock, Gulf of California Bathymetry, Mediterranean Sea Bathymetry, JODC Bathymetry, Baltic Sea Bathymetry, IBCAO Bathymetry, Caspian Sea Bathymetry, U. S. Coastal Relief Model, Great Lakes Bathymetry, Created Iceland Bathymetric Surface, SRTM30 Global Topography, GLOBE Topography, Measured and Estimated Seafloor Topography, Bathymetric pre-surface. In this process, the “mbgrid” gridding algorithm, a tight spline tension to the xyz data, based on the data hierarchy was utilized to interpolate values for cells without data. The data hierarchy follows the relative gridding weights, in which the Antarctica RAMP ice surface topography, Antarctica BEDMAP bedrock topography, the Greenland NSIDC bedrock topography datasets were given the greatest weight (Amante and Eakins, 2009). Considering the bedrock elevation data over the QTP were completely interpolated by the above-mentioned algorithm, relevant results from previous studies explained the availability of this dataset in the QTP (Thompson et al., 1989, 1990, 1995; Liu et al., 1998; Li et al., 2011). Most upland areas are composed of exposed bedrock and patchy glacier deposits. In these regions, the land and bedrock topography are in close proximity. Thicker glacier deposits are largely located in lowland areas, for which little or even no relation exists between the bedrock and land-surface topography. In grids in which the calculated bedrock elevation exceeded the surface elevation, the latter is substituted by the land-surface values (Amante and Eakins, 2009).

Shuttle Radar Topography Mission (SRTM) output on grids with a spatial resolution of 30 m (SRTM DEM 30 m) in 2001 (https://dds.cr.usgs.gov/srtm/version2_1/SRTM30/) over the QTP was collected to determine the location of the grid cell with the maximum surface elevation for individual glaciers included in RGI 4.0. In practice, the SRTM DEM 30 m is first transformed into the grids of the bedrock elevation data with the spatial resolution of 625 m by using the resampling tool based on the nearest technique to match the bedrock elevation data. The specific usage is described in Section 4. Moreover, the slope and aspect data are produced by the elevation obtained from the SRTM DEM 30 m map through the ArcGIS platform. The slope data identify the rate of maximum change in elevation from each grid. The aspect, the slope direction, captures the downslope direction of the maximum rate of change in elevation from each grid to its neighbors. In the usage, the extracted slope data were considered to keep consistent in the glacier surface during the study period. On the one hand, most glaciers in the Qinghai-Tibetan Plateau are mountain glaciers. For those located in high slopes, the surface slopes and corresponding bottom slopes are in close proximity. Therefore, even the glaciers move, the slope data hardly change (Aizen et al., 2002). While in terms of glaciers at smaller slopes, the movement of glaciers is slighter (Lambrecht et al., 2011). Considering the neighboring grids tend to be in a similar climate condition, the changes of surface elevations among these grids are in a significant synchronism when the glaciers melt (Vieli Leysinger and Gudmundsson, 2010). In general, the slope data are relatively stable. It is available to infer the glacier surface elevation distribution with them.

3.4 Glacier thickness data for validation

The World Glacier Monitoring Service (WGMS) (https://wgms.ch/) is a global program devoted to collecting and mapping glacier inventory datasets worldwide. The subset Glacier Thickness Dataset version 2.0 (GlaThiDa, http://dx.doi.org/10.5904/wgms-glathida-2016-07, doi:10.5904/wgms-glathida-2016-07) (WGMS, 2016) stores

https://doi.org/10.5194/essd-2020-71
Preprint. Discussion started: 7 September 2020

several glacier thickness measurements collected from field observations worldwide. The dataset has been structured into three data tables. The first table is the overview table (T-GLACIER THICKNESS OVERVIEW) and contains information on the location and area of the glacier, estimates of thicknesses from interpolated observations. The second table (TT-GLACIER THICKNESS DATA DERIVED FROM MAP or DEM) includes ice thickness data (mean and/or max) averaged over the surface elevation bands established based on the lower and upper boundaries from ice thickness maps or Digital Elevation Models (DEMs). The third table (TTT-GLACIER THICKNESS POINT DATA) contains point data including the elevation at the surveyed point, and the thickness value (Gärtner-Roer et al., 2014). This dataset was applied to validate in the calculated glacier thickness in the present study.

3.5 Glacier volume data for validation

The calculated glacier volumes were validated using glacier volume and change data obtained from the literature and observations. The specific information retrieved the data in the literature is listed in Table A1 (Appendix). In addition, the derivations of gravity anomaly (DGA) data over the QTP (http://www.geodoi.ac.cn/WebCn/doi.aspx?Id=539, doi:10.3974/geodb.2016.06.07.V1) (Liu et al., 2016) provide a sum of changes in soil moisture and glacier volume from 2003 to 2010 on the grids with spatial resolution of 1°, which were sourced from Gravity Recovery and Climate Experiment outputs (GRACE) (Liu et al., 2015, 2016). Soil moisture data with spatial resolution of 0.25° were extracted from the Global Land Data Assimilation System (GLDAS) products (https://ldas.gsfc.nasa.gov/gldas/, doi:10.5067/LYHA9088MFWQ) (Hiroko and Rodell, 2016) during the same period to obtain the changes in glacier volumes included in the DGA dataset. Based on these datasets, the change in glacier volume in 1°×1° pixels is calculated by subtracting the DGA value from the corresponding GLDAS soil moisture value (resampled from the 0.25°×0.25° to the 1°×1° pixel). Moreover, a newly generated estimation of global glacier ice thickness data produced by Farinotti et al. (2019) was used as an ancillary validation dataset, which was downloaded at the website "https://www.research-collection.ethz.ch/handle/20.500.11850/315707" (doi:10.3929/ethz-b-000315707). The data were developed based on the RGI 6.0, which is consistent with the GIC-II over the QTP. Thus, the glaciers with observed thickness data have also been selected from the dataset reported by Farinotti et al. (2019) and compared with the recalculated and traditional equation-based ice thickness. All of the above-mentioned data collections are listed in Table 1.

Table 1 General information about the data collections

Data types	Datasets	Usages
Input data	Randolph Glacier Inventory version 4.0 (RGI 4.0, http://www.glims.org/RGI/) The second Glacier Inventory of China (GIC-II)	Basic glacier property data (outlines, slope, aspects)
	Surface elevation data (SRTM DEM, 2001) Bedrock elevation map	Ice thickness and volume calculation
Validation data	Glacier Thickness dataset version 2.0 (https://wgms.ch/) Glacier volume data from the literature (Ma et al., 2008; Wang & Pu, 2009; Gärtner-Roer et al., 2014; Zhu et al., 2014)	Ice thickness and volume data in different space scales for validation
	Derivations of Glacier Anomaly (DGA) data (http://data.tpdc.ac.cn/),	

https://doi.org/10.5194/essd-2020-71
Preprint. Discussion started: 7 September 2020

Global Land Data Assimilation System (GLDAS) dataset
Estimation of glacier ice thickness data by Farinotti et al. (2019) (https://doi.org/10.3929/ethz-b-000315707)

4 Methods for calculating glacier volume

4.1 Ice thickness and volume determination

Because the majority of glacier data over the QTP in RGI 4.0 are obtained from the GIC-I, the recommended equation in the GIC-I is assumed to be applied to the RGI 4.0 data. In both GIC-I and GIC-II, the volume-area scaling law was based to calculate the individual glacier volume (Wu & Li, 2004; Guo et al., 2015). The following specific equations are recommended:

$$V_{\mathrm{I}} = \begin{cases} 0.0305 \cdot A^{1.11}, & A < 1\,\mathrm{km}^2 \\ 0.0542 \cdot A^{1.06}, & 1\,\mathrm{km}^2 \le A \le 3\,\mathrm{km}^2 \\ 0.0674 \cdot A^{1.16}, & A > 3\,\mathrm{km}^2 \end{cases} \tag{1}$$

$$V_{\mathrm{II}} = \begin{cases} 0.0365 \cdot A^{1.375}, & \text{maximum approximation} \\ 0.0433 \cdot \mathrm{A}^{1.29}, & \text{minimum approximation} \end{cases} \tag{2}$$

where V_{I} and V_{II} represent the glacier volume in GIC-I and GIC-II, respectively. The units of A and V are km^2 and km^3, respectively. $V_{\mathrm{I(II)}}/A$ is applied to calculate the average thickness of a glacier.

As mentioned above, data are missing from the two inventories and problems of over and underestimations of glacier volumes have been noted (Guo et al., 2015). The aforementioned datasets and the derived slope and aspect maps over in the QTP were applied to recover the missing data, determine ice thickness, and recalculate glacier volumes in the two inventories as a method to improve the accuracy of the calculations.

In addition, there is an assumption that the grid with the maximum surface elevation in an individual glacier is assumed to remain unchanged during two studied periods (Erasov, 1968; Gardelle et al., 2013; Frey et al., 2014). The following specific procedures were used:

1) Select the grid location (x_0, y_0) with the maximum elevation (Z_0) of glaciers in the RGI 4.0 using the surface elevation map constructed in 2001 (SRTM30) in the QTP.

2) Use the following slope-dependent algorithm shown below (Fig. 2) to obtain the surface elevation map based on the identified maximum elevation location (grid) identified in step 1.

① Identify the adjacent pixels of the grid with the maximum elevation recognized in step 1 (the distance between centres of two grids' at a spatial resolution of 1km is equal to or less than 1.45 km (the largest centre distance between two neighbouring pixels). These pixels are labelled as i, i=1 2, ..., n_1, with a surface elevation $Z_{1,i}$, and location ($x_{1,i}$, $y_{1,i}$)), and then calculate the surface elevation for these pixels.

$$Z_{1,i} = Z_0 - \tan(mean(slope_0 + slope_{1,i})) \times sqrt((x_{1,i} - x_0)\wedge 2 + (y_{1,i} - y_0)\wedge 2) \tag{3}$$

② Identify the adjacent pixels of the grid i identified in ①; (the found pixels are designated as j, j=1, 2, ..., n_2, with surface elevation $Z_{2,j}$, and location ($x_{2,j}$, $y_{2,j}$)).

$$Z_{2,j} = Z_{1,i} \pm \tan(mean(slope_{1,i} + slope_{2,j})) \times sqrt((x_{1,i} - x_{2,j})\wedge 2 + (y_{1,i} - y_{2,j})\wedge 2) \tag{4}$$
$$\pm: \textit{depending on the aspect comparison of grid } i \textit{ and } j$$

③ Repeat ② from i=1 to i=n_1 until the boundary pixels are identified.

https://doi.org/10.5194/essd-2020-71
Preprint. Discussion started: 7 September 2020

3) Calculate grid-based ice thickness (H) in combination with bedrock elevation map (the 1km×1km grid was used for the calculation).

$$H = Z_{2,j} - Z_{B,j} \tag{5}$$

where $Z_{B,j}$ is the bedrock elevation corresponding to $Z_{2,j}$.

4) Based on the grid-based ice thickness, the individual glacier volume was computed using the following equation:

$$V = \bar{H} \times A \tag{6}$$

where $\bar{H}$ is the pixel-averaged ice thickness.

In this process, the maximum surface elevation grid is synchronous to the grid cell of the maximum bedrock elevation (according to the correlation analysis, the correlation coefficient between the two series is greater than 0.85).

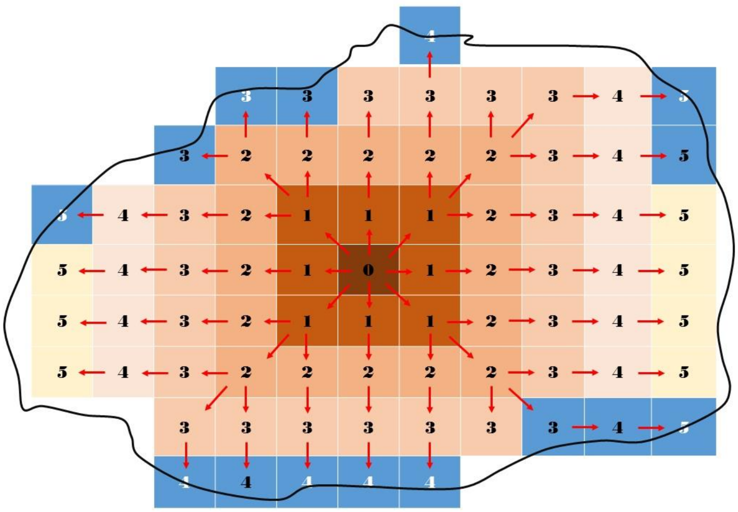

Fig. 2 Schematic map for glacier volume calculation

Note: The numbers 0-5 indicate the surface elevation of the pixels. Grids with the same number indicate a contour line.

4.2 Fragmentation index

According to previous studies, total glacier numbers have increased in recent decades, although glacier areas are significantly decreasing. The fragmentation index introduced in landscape-related studies was adopted and computed using the following equation to analyse the changes in glacier numbers in different areas during the past few decades:

$$FI_i = \frac{N_{\text{GIC-II},i} / N_{\text{RGI 4.0},i} - 1}{\left(\sum_{t=1}^{N_{\text{RGI 4.0}}} A_{\text{RGI4.0},i,t} / \min(A_{\text{RGI 4.0},i})\right) / \left(\sum_{t=1}^{N_{\text{GIC-II}}} A_{\text{GIC-II},i,t} / \min(A_{\text{GIC-II},i})\right)} \tag{7}$$

where i (i=1, 2, 3, ..., 11) represents the code for different mountains. FI_i is the fragmentation index of i. $N_{\text{RGI 4.0},i}$

https://doi.org/10.5194/essd-2020-71
Preprint. Discussion started: 7 September 2020

and $N_{\text{GIC-II},i}$ refer to the glacier number of mountain i in RGI 4.0 and GIC-II, respectively. $A_{\text{RGI 4.0},i,t}$, $A_{\text{GIC-II},i,t}$ are the area of the glacier t in mountain i in RGI 4.0 and GIC-II, respectively. $\min(A_{\text{RGI 4.0},i})$ and $\min(A_{\text{GIC-II},i})$ mean the minimum glacier area in mountain i in RGI 4.0 and GIC-II, respectively.

A higher fragmentation index indicates that more surfaces are exposed to sunlight, which might result in more energy accepted by glaciers to produce more meltwater. Meanwhile, the shear stress would also increase and basal sliding would accelerate, which is the key interpretation of how the glacier movement and deformation will develop.

In addition, the ratio of disintegrated glaciers (RDG) is computed as follows.

$$\text{RDG}=\frac{\text{GIC-II\_GN}-\text{RGI 4.0\_GN}+\text{Disappeared\_GN}-\text{Surged\_GN}}{\text{RGI 4.0\_GN}} \tag{8}$$

where RGI 4.0_GN, GIC-II_GN are the glacier number in RGI 4.0 and GIC-II, respectively. Disappeared_GN and Surged_GN indicate the number of disappeared and surged glacier number from the 1970s to the 2000s, respectively.

The following equation was used to calculate the average number of glaciers in the GIC-II that disintegrated from a glacier in the RGI 4.0.

$$\text{DGN}=\frac{\text{GIC-II\_GN}-\text{Surged\_GN}}{\text{RGI 4.0\_GN}-\text{Disappeared\_GN}} \tag{9}$$

where DGN presents the glacier number that disintegrated from the RGI 4.0 to GIC-II.

4.3 Uncertainty estimation

According to a large amount of statistics, approximately half area of boundary pixels are included in the glacier. In the practical calculation, the whole area of boundary pixels is counted in the glacier volume. Thus, the product of the number of boundary pixels and half area of each pixel is computed to quantify the uncertainty in the glacier area using the following equation (Shi et al., 2009; Guo et al., 2015).

$$\varepsilon = N \cdot A' \tag{10}$$

where N is the number of boundary pixels and A' is the half area of each pixel. The individual glacier volume is finalized as the range of $(A\pm\varepsilon)\cdot H$ to include the uncertainty in the glacier area.

5 Results

5.1 Validation of the calculated ice thickness and volume

Using the input data and the methods specified above, the ice thickness and volume of individual glaciers are calculated. The calculated values for selected glaciers are compared with the observed data and corresponding equation-based results in RGI_4.0 and GIC_II (Fig. 3). Most of the calculated glacier volumes display better agreement with observations than the equation-based results for the selected glaciers, particularly in the Nyainqentanglha Mountains (Bayi and Gurenhekou Glaciers). While at the Shule_5 and Shule_6 glaciers in the northern Qilian Mountains, both calculated and equation-based thickness and volume values are much larger than the observed values in the RGI 4.0. In the GIC-Ⅱ, Farinotti et al.'s (2019) results tend to be lower than the other two values. In general, errors in the provided slope-dependent algorithm are smaller than errors for the equation. Therefore, it will be further used to calculate all individual glacier volumes in RGI 4.0 and GIC-Ⅱ. The relevant

https://doi.org/10.5194/essd-2020-71
Preprint. Discussion started: 7 September 2020

descriptions are provided below.

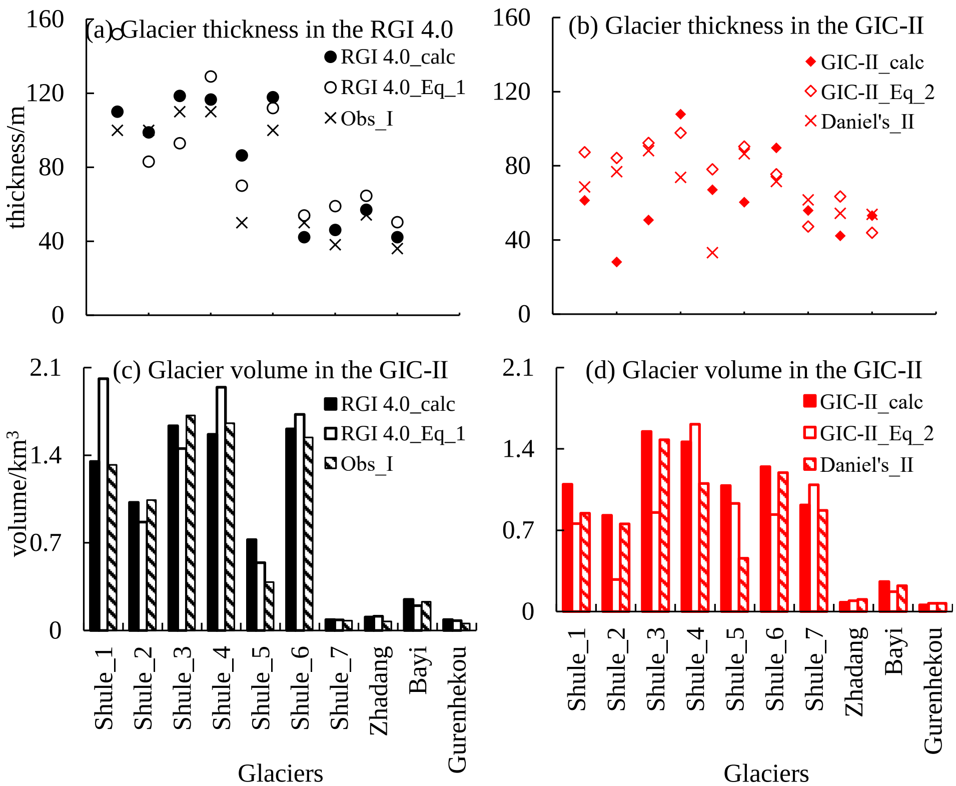

Fig. 3 Comparisons between observed glacier volumes and values calculated using different methods

Note: The ice thickness values are reported as average values. RGI 4.0_calc, RGI 4.0_Eq_1, and Obs_I are the calculated, Eq. (1)-based, and observed values in the RGI 4.0, respectively. GIC-Ⅱ_calc, GIC-Ⅱ_Eq_2 and Daniel's_Ⅱ represent the calculated, Eq. (2)-based values (the averages of the minimum and maximum values), and Farinotti et al.'s (2019) results obtained by averaging five types of glacier model outputs in the GIC-Ⅱ.

Three GRACE data grids with a spatial resolution of 1° (approximately 100 km×100 km) from the Himalayan Mountains are also chosen to further compare and validate the calculated results and products of glacier volume change as shown in Table 2. An underestimation is observed in the results obtained with the volume-area scaling. In particular, the approximately 45.6%~58.4% rate of change in the total glacier volume has been underestimated by Eq. (2) during 2003-2009 on the west-most grid, but an underestimation of only 10.4% in the change in the total glacier volume occurs using the slope-dependent method. Moreover, a large extent of change in the glacier volume is given by the empirical equation for the central pixel selected, and, fortunately, the observed result is similar to the peak value of the range. In the eastern pixel, a ratio of 16.8-22.4% of change in the observed glacier volume change has been identified from the results of the volume-area scaling, while the calculation produces an overestimation of 6.5% in the DGA-derived change in the glacier volume.

https://doi.org/10.5194/essd-2020-71
Preprint. Discussion started: 7 September 2020

Table 2 Changes in glacier volume during 2003-2009/2010 in the selected DGA data grids

Central-lon	Central-lat	Period	Calculated glacier volume change km^3	Equation-based glacier volume change km^3	DGA-derived glacier volume change km^3
86	28	2003-2009	22.4	10.4~13.6	25
87	28	2003-2010	8	1.9~8.9	8
88	28	2003-2010	11.4	8.3~8.9	10.7

The calculated results are also compared with relevant studies in the QTP presented in the literature (Table 3). All selections have similar study periods with the corresponding information in the RGI 4.0 and GIC-Ⅱ, from which the change in the glacier volume in the Gongga Mountains located in the Hengduan Mountains is overestimated by the volume-area scaling because of the significant underestimation of the glacier volume in the GIC-Ⅱ. Meanwhile, changes in the glacier volume in the central Nyainqentanglha Mountains and Dongkemadi Glacier in the Tangula Mountains are underestimated by the traditional method due to the overestimation of glacier volume in the GIC-Ⅱ. In addition, the results for the Laohugou No.12 Glacier in the Qilian Mountains calculated using the slope-dependent and volume-area scaling are consistent mainly because the equation was determined based on the observations over the surrounding area. In general, the comparison of the results reveals good agreement with the verifications conducted above.

Table 3 Comparison with changes in the observed glacier volume reported in the literature

Region	Period	Location/code	Observed volume change in references (km^3)	Calculated volume change (km^3)	Equation-based volume change (km^3)
Gongga Mountains	1966-2015	29°-30° N, 101°-102°E	-1.65 (Cao et al., 2019)	-1.06	-5.99
Central Nyainqentanglha Mountains	1968-2000	30.15°-30.88° N, 94°-95.5° E	-23.62 (Brun et al., 2017; Wu et al., 2019)	-17.32	-8.23
Dongkemadi Glacier	1969-2000	5K443D0038	-1.17 (Li et al., 2012)	-1.32	-0.09
Laohugou No.12 Glacier	1957-2007	5Y448D0012	-0.22 (Liu et al., 2018; Zhang et al., 2012)	-0.28	-0.5

5.2 Changes in volumes

The individual glacier volume equals the pixel-averaged ice thickness multiplied by the area (Eq. (6)). The sums of individual glacier volumes in the recalculated RGI 4.0 and GIC-II inventories are provided in Table 4. The total area of glaciers in the QTP extracted from the RGI 4.0 is approximately 54874.79 km^2, and the area extracted from the GIC-II is 43745.48 km^2, representing a decrease of 11129.31 km^2. The total glacier volume was reduced from

https://doi.org/10.5194/essd-2020-71
Preprint. Discussion started: 7 September 2020

4716.76 km^3 in the RGI 4.0 to 4045.59 km^3 in the GIC-II. The results suggest a significant retreat and melting of glaciers in the QTP since the 1970s.

The glacier volumes of the Tangula Mountains, Qiangtang Plateau, Karakoram and Kunlun Mountains in the inland Tibetan Plateau are lower than volumes calculated with the volume-area scaling (Table 4). However, the calculated volumes for the other mountains are larger than the equation-based values. In the compilation of Glacier Inventory of China, the traditional empirical equations were determined by the survey and monitoring on glaciers from northern mountains, particularly in the eastern Qilian Mountains where lack extensive deep valleys (Liu et al., 2003; Wu & Li, 2004; Shangguan et al., 2010). Thus, the total glacier volume in the Qilian Mountains is underestimated. However, the inland Tibetan Plateau is filled with more flatter lands. This difference may cause the overestimation of glacier volume in the inland Tibetan Plateau using the empirical area-volume equations determined without enough available field observations in this area. Weakening of the westerlies and the Indian Summer Monsoon might be the dominant factors limiting glacier accumulation in recent decades (Yao et al., 2012b). On the other hand, the geological structure of the southwestern mountains tends to be more complicated with a large number of deep valleys due to several gigantic orogenic movements in history. The higher mountains with deeper valleys store thicker glaciers, leading to the underestimation of glacier volume by the volume-area scaling in these areas. The causation is that deep valleys tend to store thicker glaciers, but lack observations (Guo et al., 2015). Thus, the empirical equations cannot capture the information for these areas so the underestimation is always bound. Moreover, traditional empirical equations tend to underestimate glacier volumes for small glaciers (an area of less than 1 km^2), as well as parts of large glaciers with thin layers (an area greater than 10 km^2 and thickness less than 40 m). Thus, most of the equation-based glaciers volumes are median in scale, while small glaciers and large glaciers with thin layer always have a lower proportion of the volume to area ratio (Klein et al., 2014; Wang et al., 2019).

Table 4 Comparison of the calculated and equation-based glacier volumes in different mountains

Mountains	Glacier volume in RGI 4.0 (km^3)		Glacier volume in GIC-II (km^3)		Changing rate of glacier volume based on calculations (%)
	Calculation	Equation 1	Calculation	Equation 2	
Altin	31.69	22.02	29.83	15.36	-5.86
Pamir	249.35	221.10	281.66	166.32	+12.96
Hengduan	200.88	175.93	131.27	77.03	-34.65
Qilian	185.64	140.58	135.90	84.48	-26.79
Tangula	178.72	229.97	123.59	140.25	-30.85
Gandise	197.07	164.75	96.01	55.79	-51.28
Qiangtang	192.92	254.26	136.93	166.93	-29.02
Himalaya	705.29	618.48	603.92	497.66	-14.37
Karakoram	501.81	553.40	524.87	589.32	+4.59
Nyainqentanglha	1065.71	981.16	937.65	859.36	-12.02
Kunlun	1207.68	1260.06	1044.18	1117.96	-13.54

Note: The results listed in "Equation 1" are obtained from Eq. (1). The results listed in "Equation 2" are based on the averages of the minimum and maximum values calculated using Eq. (2).

https://doi.org/10.5194/essd-2020-71
Preprint. Discussion started: 7 September 2020

The comparison of the recalculated RGI_4.0 and GCI_II indicates that the glacier areas of all mountains over the QTP have decreased in the past 4 decades. The smallest percent reduction in glacier area is observed in the Altin Mountains, with the value of approximately 8.26% of the total area. In the Gandise Mountains, the glacier area over all aspects has decreased to 45.36% of its total area, which is the largest percent reduction in glacier area among all the studied mountains. Meanwhile, the change in the glacier volume in the Gandise Mountains is consistent with the change in glacier area, i.e., it also exhibits the largest percent decrease of －51.28% (Table 4). However, the Tangula Mountains contain an area of expansion on the northwestern aspect, while the glacier area increased on the southwestern aspect in the Pamir and Qiangtang Plateaus. In addition, the increase in the glacier area in the other mountains is mainly located on the northern and northeastern aspects. The majority of advancing glaciers are distributed in the northwestern Karakoram Mountains with higher rate than other mountains. The results are consistent with the study by Liu et al.'s (2014).

5.3 Disappeared and surged glaciers from 1970s to 2000s

The glacier information in the calculated RGI 4.0 and GIC-II is compared to detect the disappeared and surged glaciers with the aid of the ArcGIS toolbox (Fig. 4). The disappeared glaciers refer to glaciers that were included in the RGI 4.0 but did not appear in the GIC-II. The surged glaciers include the glaciers that were emerging in the GIC-II. The statistical analyses of the disappeared and surged glacier numbers and volumes over different mountains are displayed in Fig. 5. The Karakoram and Kunlun Mountains have comparably larger numbers of surged glaciers, with values of 1598 and 1329, respectively. However, the Gandise and Himalayan Mountains contain the greatest numbers of disappeared glacier at 1405 and 1387, respectively. The results are consistent with the study by Bhambri et al.'s (2017).

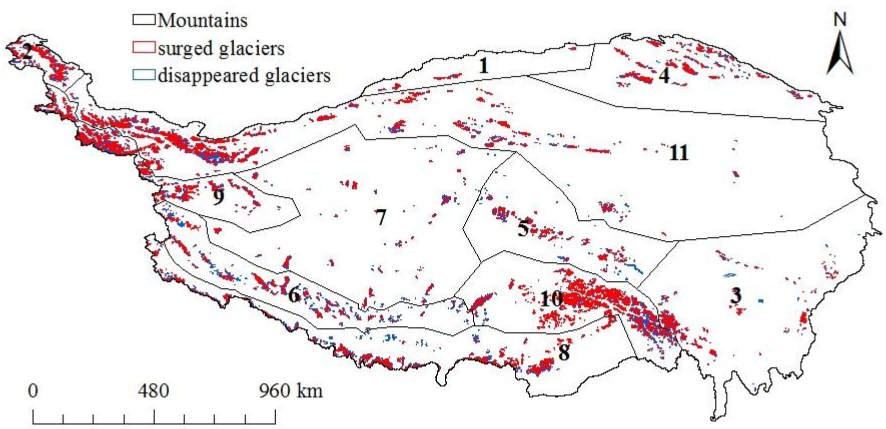

Fig. 4 Disappeared and surged glaciers from the 1970s to 2000s over the QTP

https://doi.org/10.5194/essd-2020-71
Preprint. Discussion started: 7 September 2020

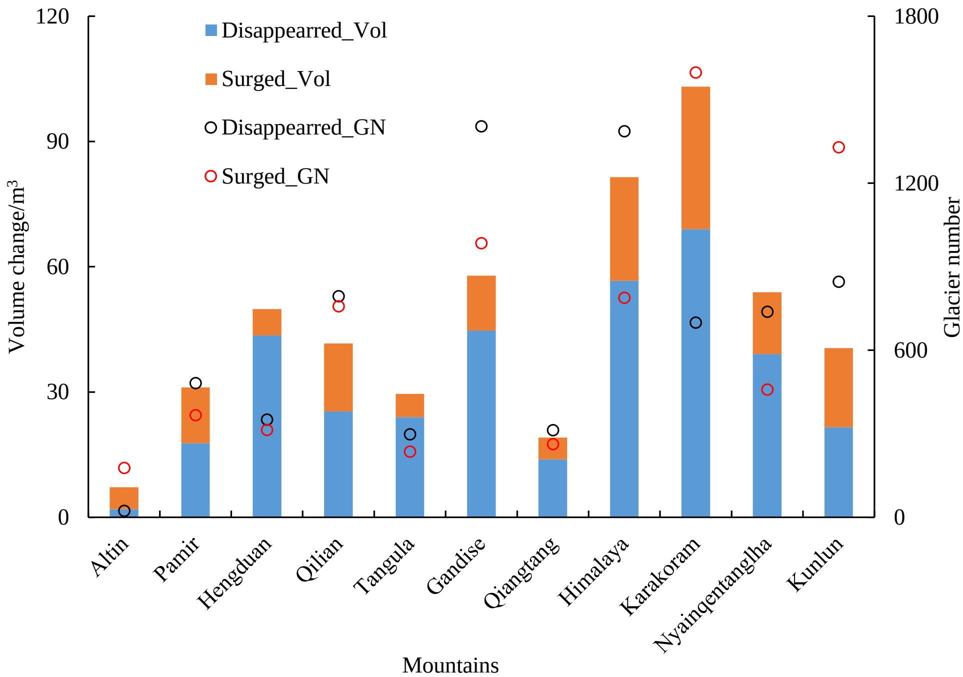

Fig. 5 Statistical analyses of disappeared and surged glaciers in 1970s and 2000s in the QTP

Note: Disappeared_Vol, Surged_Vol refer to the disappeared and surged glacier volume from the 1970s to the 2000s, respectively.

5.4 Effects of mountain directions on changes in glacier volumes in the RGI 4.0 to GIC-II

In the QTP, different mountains run in different directions (Fig. 5) and different aspects have different climatic conditions, causing diverse glacier accumulation and ablation. In the context of climate change, the advance and retreat of glaciers may vary in the different aspects of each mountain. Therefore, studies exploring changes in glacier volume in different aspects are necessary to understand the mechanisms by which the changing climate and monsoon affect the glaciers. The glacier volumes in the recalculated RGI 4.0 and GIC-II are summed for different mountains to investigate the variations (Fig. 6). The changing pattern of glacier volume in the Nyainqentanglha Mountains is similar to the Himalayas. A similar pattern of changes is also observed in the Qilian, Kunlun and Gandise Mountains. The Altin Mountains have experienced a significant increase on the northern (0°-15° and 345°-360°) aspect and slight increase on the eastern (75°-105°), south-southeastern (SSE, 135°-165°), north-northwestern (NNW, 315°-345°) aspects. The Pamir Plateau displays a significant increase in glacier volume on the east-southeastern (ESE, 105°-135°), north-northeastern (NNE, 15°-45°), west-southwestern (WSW, 225°-255°) and west-northeastern (WNW, 285°-315°) aspects, while the glacier volumes decreased on other aspects. In addition, the glacier volumes in the Hengduan Mountains and Himalayan Mountains have undergone an increase in the eastward direction. The Qilian Mountains display an increase in glacier volume on the northern and NNE aspect. The total glacier volume in the Karakoram Mountains increased on the northern aspect. The glacier volume on the northern and NNE aspects underwent an increase in the Kunlun Mountains. Moreover, the Nyainqentanglha Mountains exhibit an increase in glacier volume on the eastern aspect. The Qiangtang Plateau displays a slight increase in the glacier volume on the east-northern aspect. However, the glacier volumes at all aspects in both the Tangula and Gandise Mountains were reduced during the study period. On the other hand, the statistics of glacier volume changes on different aspects described above reflect glacier movement.

In summary, the volume of glaciers in most of mountains decreased on the western and southern aspect in the studied period. The aspects displaying a reduction in glacier volume in the northern mountains are concentrated on the northern and northeastern aspect, while the southern mountains mainly exhibit a decrease in glacier volume on the eastern and even a few southeastern aspects. Thus, the concentrations of aspects of the mountains with increasing glacier volumes from north to south are shifting from north and northeast to east and southeast, indicating that glacier retreat occurs in the southwestern aspects of mountains, while the northeastern aspects of mountains tend to display glacier advance.

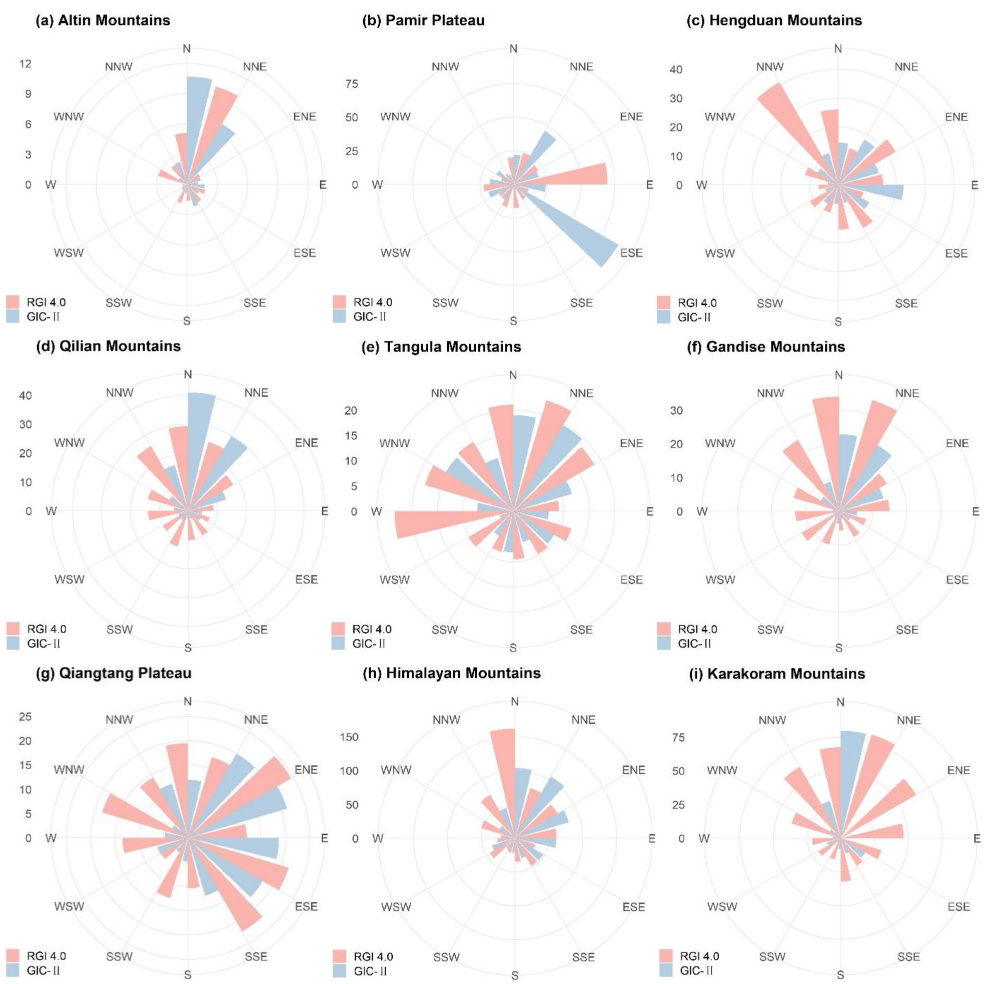

https://doi.org/10.5194/essd-2020-71
Preprint. Discussion started: 7 September 2020

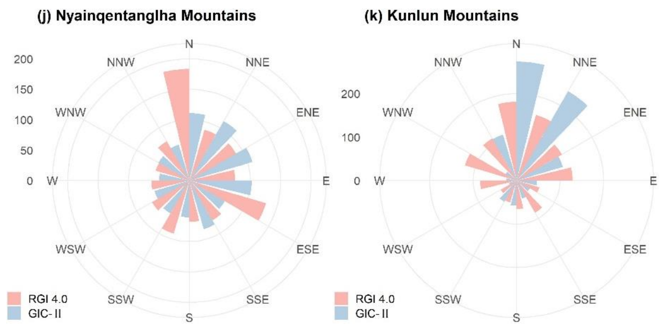

Fig. 6 Glacier volumes on different aspects of eleven mountains in calculated RGI 4.0 and GIC-II (unit: km^3)

Note: The statistical analyses of glacier volumes in each mountain are conducted on twelve direction ranges (anticlockwise is defined as positive direction; due north is 0°). For instance, the range of 15°-45° refers to the north-northeast orientation (NNE). Areas of the fan-shaped sector coloured in red and blue represent the glacier volumes in the calculated RGI 4.0 and GIC-II, respectively.

5.5 Glacier fragmentation

Glacier melting can lead to the disappearance of small glaciers and the fragmentation of a part of large glaciers (Liu et al., 2014). To quantify such fragmentation, the fragmentation indexes of glaciers in different mountains from RGI 4.0 to GIC-II are calculated using Eq. (7). The results are shown in Fig. 7. It is obvious the values of fragmentation index are either positive or negative, which directly depend on the change of glacier number from RGI 4.0 to GIC-II in different mountains. The larger the fragmentation index is, the greater glacier number in GIC-II has, or the smaller decrease of glacier area from the RGI 4.0 to GIC-II occurs. Specifically, the value of fragmentation index in the Altin Mountains is largest with the number over 0.8, indicating the highest degree of fragmentation. The inferior value of fragmentation index appears in the Karakoram Mountains at 0.41. Both are observed with a significant increase in glacier number from the RGI 4.0 to GIC-II, whereas the decreases of glacier area in the period are slight. In addition, the Kunlun Mountains, Qiangtang Plateau, Qilian Mountains, Hengduan Mountains, Nyainqentanglha Mountains and Tangula Mountains are observed with positive values of fragmentation index, in which the Qiangtang Plateau and Hengduan Mountains not only have an increasing glacier number, they also experienced an apparent decrease of area in glaciers from the RGI 4.0 to GIC-II. Moreover, the Gandise Mountains, Pamir Plateau, and Himalayan Mountains are calculated with negative fragmentation indexes. The Gandise Mountains went through little decrease in glacier number, while the decrease of area in glaciers is largest over the studied mountains from the RGI 4.0 to GIC-II.

The ratio of separated glaciers was calculated using Eq. (8) to quantify the glacier number with separation in each mountain. Approximately 29.7% of glaciers in the Qiangtang Plateau have separated into pieces, which is the highest ratio of glaciers with separation among all the studied mountains. On average, every glacier in the Qiangtang from the RGI 4.0 disintegrated into approximately 1.4 sub-glaciers in the GIC-Ⅱ, as calculated using Eq. (9), which is also the largest number over all mountains. The glaciers formed from the disintegrated glaciers in the RGI 4.0 account for 10-15% of the total glacier number in GIC-II in more than half of the studied mountains, while the Pamir Plateau and Himalayan Mountains only contain approximately 3.4% and 4.4% of split glaciers, respectively. The causes of glacier separation differ from the maritime-type and continental

Open Access Earth System Science Data Discussions

glaciers. For the maritime glaciers, the ocean current, the strength of wind and self-melting all induce and even accelerate glacier fracture. In the continental glaciers, topographical, geological and climate changes are the dominant factors contributing to the deformation of glaciers.

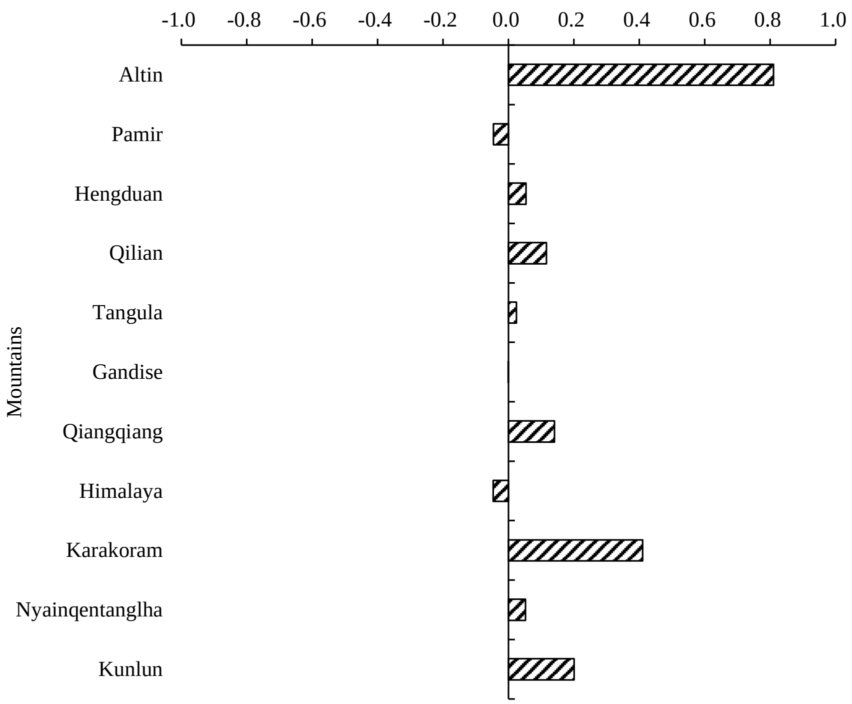

Fig. 7 Fragmentation indexes of the glaciers in different mountains

6 Uncertainties in the recalculated inventories

6.1 Uncertainty of input data

Glaciers in the study area are divided into two types, including maritime and continental glaciers. The greatest difference in the two types is the summer accumulation- and winter accumulation-dominated patterns, respectively (Huang, 1990; Shi and Li, 1981). The maritime glaciers are mainly distributed in the southeastern Tibetan Plateau, while the continental type of glaciers is generally distributed in the other areas. Typically, more extensive snow and cloud cover exist during ablation seasons (winter for the maritime glaciers and summer for the continental glaciers), leading to the inconsistency of glacier outline in the same map. This inconsistency is one source of uncertainty in the recalculated inventories. Regarding the image sources used in this study, some glaciers (14%) were mapped in winter (November to March), while the remaining 86% of glacier maps were acquired from April to October (summer). Thus, the technology used to extract the snow and cloud cover from the original images is important to efficiently determine the ice coverage. The accuracy of glacier delineation is mainly determined by seasonal snow around the ice margin or within the debris-covered area, and by cloud cover over the glacier surface. In practice, a value of 2.0 was set as the threshold for TM3/TM5 to differentiate snow within a five-pixel buffer of the glacier outline and debris-covered area (greater than 2.0), and cloud cover within the clean-ice area (less than 2.0). Notably, 86% of images have 20% snow/cloud coverage, in which approximately 48% of images have snow/cloud cover of less than 10%. The lower-quality images (snow/cloud coverage greater than 20%) are mainly concentrated in the western Himalayan region (30-32°N, 77-81°E) and Kunlun Mountains (36°N), whereas the inland Tibetan Plateau (33-35°N, 84-90°E) displays the best image quality (Li, 1986; Pu, 2001; Mi et al., 2002). According to the statistics, 1494 km^2 out of the total area of 43087 km^2 are debris-covered surfaces (Guo et al., 2015).

On the other hand, many studies have suggested that the vertical accuracy of the TOPO DEM (30 m grid cell) used in the GIC-I is better than 11 m on glaciers with mean slopes <24° (Chinese National Standard, 2008; Shangguan et al., 2010; Wei et al., 2015; Xu et al., 2013; Zhang et al., 2016). However, the slopes of more than 2×10^4 km^2 of glaciers are greater than 24°, which may result in a larger uncertainty. In addition, the glacier outlines in the GIC-II were mapped using several different satellite images, including the SRTM DEM acquired by the radar interferometry with C-band and X-band in early February 2000 (Rabus et al., 2003; Zwally et al., 2011), the 1 arc-second SRTM C-band DEM, the non-void-filled SRTM C-band DEM with a swath width of 225 km (http://earthexplorer.usgs.gov/) TerraSAR-X (June 2007) and its twin satellite TanDEM-X (June 2010) launched by the German Aerospace Center (DLR) (Hajnsek et al., 2007), etc. The difference in projection angle, collection period and pixel layout in data sources are other sources of uncertainty in the recalculated inventories, which must be improved in the future related studies. In addition, uncertainty is unavoidably bound with using the extracted slope data from the SRTM DEM 30 m map in 2001 to present the slope distribution in both RGI 4.0 and GIC-Ⅱ (Jiskoot and Mueller, 2012). Further exploration on this uncertainty is also needed.

6.2 Inconsistency of data source dates in the same glacier map

Different glacier information was interpreted by different images collected in the 1970s or the 2000s. The direct generalization and comparison may cause some bias in the results. Specifically, 84.34% of the images in the RGI 4.0 were collected between 1956 and 1980, and 12.27% of them were collected from 1981 to 2008, while 3.37% of the collected years were missing and one of the images was obtained from 1920. Regarding the data sources of glaciers in the GIC-II, 84.55% of images were collected in the period from 2004 to 2011. Notably, 15.01% of images were collected from 1958 to 1980. Additionally, the source dates of the remaining 0.44% of images were missing. Moreover, the information for a number of glaciers in the southeastern Tibetan Plateau have not been updated in the GIC-II. However, they were treated as being from the same year in this study to simplify quantitation. No updated images for a number of glaciers over the southeastern QTP were available in the GIC-II, and thus the information in the RGI 4.0 was used. Therefore, the comparison of the results between the two inventories should be interpreted with caution.

6.3 Inconsistency of the boundary pixel size in glacier volume calculation

An assumption in volume calculations is that all grids inside a glacier have the same size. In fact, the border of glaciers is always curved, and thus the boundary grids with the centre inside are partially included while those without the centre inside are excluded in the glacier thickness estimation. However, these boundary grids are treated as the same size to obtain the overall average thickness of a glacier. Thus, another source of uncertainty in the calculation is derived from the boundary pixel size. The error range has been obtained using Eq. (10) to estimate

https://doi.org/10.5194/essd-2020-71
Preprint. Discussion started: 7 September 2020

the impact of uncertainty in glacier area induced by boundary pixels on the calculated glacier volume (Table 5). The Qiangtang Plateau and Tangula Mountains have the largest errors of over 6% in the RGI 4.0. In the meantime, both errors are greatest in the GIC-Ⅱ with the values of 6.68% and 5.8%, respectively. However, the Pamir Plateau has the smallest error in both RGI 4.0 and GIC-Ⅱ at 3.96% and 2.84%, respectively. Most of the errors in other mountains range from 4~5%.

In addition, another comparison of the equation-based and calculated glacier volumes in the eleven mountains has been conducted and the results are presented in Table 5. The results of the RGI 4.0 indicate that the majority of values obtained using empirical equations are consistent with the error ranges of the calculation, in which only the Qiangtang Plateau displays a slight discrepancy. A small overestimation of the empirical equation exists in the Qiangtang Plateau. In addition, the glacier volumes in the Altin Mountains, Pamir Plateau, Hengduan, Qilian and Gandise Mountains are underestimated by the volume-area scaling in the GIC-Ⅱ.

Table 5 Error estimates of the calculated glacier volumes

	Glacier volume in RGI 4.0				Glacier volume in GIC-II				
Mountains	Calc_high limit (km^3)	Calc_low limit (km^3)	Eq. (1) - based values (km^3)	Error rate/ %	Calc_ high limit (km^3)	Eq. (2) - based high limit (km^3)	Calc_ low limit (km^3)	Eq. (2) - based low limit (km^3)	Error rate/ %
Altin	33.21	30.16	24.50	4.81	31.12	16.00	28.54	14.71	4.32
Pamir	259.23	239.46	234.08	3.96	289.65	171.62	273.67	161.02	2.84
Hengduan	209.30	192.46	136.39	4.19	136.23	79.48	126.31	74.57	3.78
Qilian	194.47	176.81	140.93	4.76	141.58	87.60	130.22	81.35	4.18
Tangula	189.91	167.53	191.64	6.26	130.76	141.96	116.43	138.54	5.80
Gandise	206.17	187.96	108.54	4.62	99.31	59.27	92.71	52.30	3.44
Qiangtang	205.73	180.11	234.04	6.64	146.07	169.65	127.79	164.21	6.68
Himalaya	736.09	674.49	643.63	4.37	628.31	505.74	579.52	489.57	4.04
Karakoram	528.67	474.96	554.25	5.35	547.07	623.79	502.66	554.84	4.23
Nyainqentanglha	1112.14	1019.29	971.96	4.36	976.52	891.88	898.35	826.83	4.17
Kunlun	1262.57	1152.80	1459.86	4.54	1089.72	1174.19	998.63	1061.73	4.36

7 Challenges and expectations for future studies

Glacier formations in different mountains display substantial discrepancies due to the special topographic, geological and geomorphologic conditions. These discrepancies result from several crustal movements occurring from the northern to southern QTP in different historical periods. Therefore, the unified equation is not always suitable for all of these mountains. Additional field survey results and observations must be collected to improve the quality of the bedrock elevation database and increase the accuracy of glacier volume calculation. More accurate surface elevation information is also important. However, a large gap still exists to interpret the

https://doi.org/10.5194/essd-2020-71
Preprint. Discussion started: 7 September 2020

information obtained from the remote sensing images of surging glaciers (Gardner et al., 2013; Kääb et al., 2014; Neckel et al., 2014). Therefore, the algorithm used to calculate the cloud- and debris-covered areas and derive a finer glacier outline must be strengthened based on the overwhelming number of remote sensing images and corresponding products. In addition, due to the lack of field observations of glaciers in the southeastern Tibetan Plateau, a more complete use of relevant materials to recover the current glacier information and update the GIC-II are also substantial challenges but important needs. Moreover, uncertainty quantifications must be further developed. In the future related studies, the error range should also be reduced to more precisely understand the actual state of the glacier.

8 Data availability

The data are available under https://doi.org/10.11888/Glacio.tpdc.270390 (Liu, 2020). For the time of review, the data will be accessible through the following review link https://data.tpdc.ac.cn/en/data/4b88e394-0eb4-44c4-aa38-32aeb614daff/.

9 Conclusion

We provided a set of recalculated data for all glaciers over the QTP in the RGI 4.0 and GIC-II inventories using a slope-dependent algorithm based on several elevation datasets. The two recalculated glacier inventories were compared in the eleven major mountains to investigate glacier changes in the context of climate change during the past few decades. The main results are summarized below.

(1) The glacier volumes calculated using the slope-dependent algorithm perform better than the traditional area-volume-based equations. The glacier volumes in the inland Tibetan Plateau have been overestimated by the traditional method, while the glacier volumes in the western and southern mountains tend to be underestimated.

(2) The value of fragmentation index in the Altin Mountains is largest, indicating the highest degree of fragmentation. The Karakoram Mountains and Kunlun Mountains have comparably larger fragmentation indexes, suggesting a stronger effect of climate changes on the glaciers in these mountains.

(3) Most of the surging glaciers are observed in the Karakoram and Kunlun Mountains, while the Gandise and Himalayan Mountains contain the greatest number of disappeared glaciers during the study period. In addition, the largest glacier volume loss appears in the Karakoram and Himalayan Mountains. The Karakoram Mountains also exhibit the largest surged glacier volume.

(4) An obvious offset of glacier volumes between different aspects is observed in most mountains. In general, the glaciers on the western and southern aspects displayed a greater reduction in volume in the studied period. Glaciers with increased volumes are mainly located on the northern and northeastern aspects in the northern mountains, while the southern mountains have surging glacier volumes on the eastern and southeastern aspects.

https://doi.org/10.5194/essd-2020-71
Preprint. Discussion started: 7 September 2020

Author contributions. Data collection and preprocessing: X.L., H.Y., Z.X., C.G., R., Q.Y.; Supervision: H.Y., Z.X.; Writing-original draft: X.L. and H.Y.; Writing-review and editing: X.L., H.Y. and Z.X.

Competing interests. The authors declare no conflicts of interest.

Acknowledgement. The work is financially supported by the State Key Program of National Natural Science of China (91647202). The authors are grateful to data providers. We thank Andreas Scheidegger, and Reynold Chow for the cooperation.

References

Aizen, V., Aizen, E., and Nikitin, V. N.: Glacier regime on the northern slope of the Himalaya (Xixibangma glaciers), 97-98, 27-39, https://doi.org/10.1016/S1040-6182(02)00049-6, 2002.

Amante, C. and Eakins, B. W.: ETOPO1 1 Arc-minute Global Relief Model: Procedures, data sources and analysis. NOAA Technical Memorandum NESDIS NGDC-24, National Oceanic and Atmospheric Administration, National Environmental Satellite Data, and Information Service, National Geophysical Data Center, Boulder, Colorado, 2009.

Benn, D. I., Bolch, T., Hands, K., Gulley, J., Luckman, A., Nicholson, L. I., Quincey, D., Thompson, S., Toumi, R., and Wiseman, S.: Response of debris-covered glaciers in the Mount Everest region to recent warming, and implications for outburst flood hazards (elevation changes on glacier surface, ice velocity, mass balance), Earth-Science Reviews, 114, 156-174, https://doi.org/10.1016/j.earscirev.2012.03.008, 2012.

Bhambri, R., Bolch, T., Kawishwar, P., Dobhal, D. P., Srivastava, D., and Pratap, B.: Heterogeneity in glacier response in the upper Shyok valley, northeast Karakoram, The Cryosphere, 7, 1385-1398, https://doi.org/10.5194/tc-7-1385-2013, 2013.

Bhambri, R., Hewitt, K., Kawishwar, P., and Pratap, B.: Surge-type and surge-modified glaciers in the Karakoram, Scientific reports, 7, 15391, https://doi.org/10.1038/s41598-017-15473-8, 2017.

Bolch, T.: Climate change and glacier retreat in northern Tien Shan (Kazakhstan/Kyrgyzstan) using remote sensing data, Global and Planetary Change, 56, 1-12, https://doi.org/10.1016/j.gloplacha.2006.07.009, 2007.

Bolch, T. T., Yao, T. D., Kang, S., Buchroithner, M. F., Scherer, D., Maussion, F., Huintjes, E., and Schneider, C.: A glacier inventory for the western Nyainqentanglha Range and Nam Co Basin, Tibet, and glacier changes 1976-2009, The Cryosphere, 4, 419-433, https://doi.org/10.5194/tc-4-419-2010, 2010.

Brun, F., Berthier, E., Wagnon, P., Kääb, A., and Treichler, D.: A spatially resolved estimate of High Mountain Asia glacier mass balance from 2000 to 2016, Nat. Geosci., 10, 668-673, https://doi.org/10.1038/ngeo2999, 2017.

Cao, B., Pan, B. T., Guan, W. J., Wen, Z. L., and Wang, J.: Changes in glacier volume on Mt. Gongga, southeastern Tibetan Plateau, based on the analysis of multi-temporal DEMs from 1966 to 2015. Journal of Glaciology, 65, 366-375, https://doi.org/10.1017/jog.2019.14, 2019

Che, Y. J., Zhang, M. J., Li, Z. Q., Wang, S. J., Du, M. X., Wang, P. Y., Wang, J., and Zhou, P. P.: Quantitative evaluation of glacier change and its response to climate change in the Chinese Tien Shan, Cold Regions Science and Technology, 153, 144-155, https://doi.org/10.1016/j.coldregions.2018.05.010, 2018.

Chinese National Standard (GB/T 12343.1-2008). (Eds.): Compilation specifications for national fundamental scale maps. Part 1: Compilation specifications for 1:25000/1:50000/1:100000 topographic maps, General Administration of Quality Supervision, Inspection and Quarantine, Beijing, 2008. [in Chinese]

Deng, C. and Zhang, W. C.: Spatial distribution pattern of degree-day factors of glaciers on the Qinghai-Tibetan Plateau. Environ. Monit. Assess., 190, 474-483, https://doi.org/10.1007/s10661-018-6860-7, 2018.

Erasov, N. V.: Method to determine the volume of mountain glaciers (in Russian), Data of Glaciological Studies, 14, 307-308, 1968. [in Russian]

Farinotti, D., Brinkerhoff, D. J., Clarke, G. C., Fürst, J. J., Frey, H., Gantayat, P., Chaulet, F. G., Girard, C., Huss, M., Leclercq, P. W., Linsbauer, A., Machguth, H., Martin, C., Maussion, F., Morlighem, M., Mosbeux, C., Pandit, A., Portmann, A., Rabatel, A., Ramsankaran, R., Reerink, T. J., Sanchez, O., Stentoft, P. A., Kumari, S., Pelt, W. J. J. V., Anderson, B., Benham, T., Binder, D., Dowdeswell, J. A., Fisher, A., Helfricht, K., Kutuzov, S., Lavrentiev, I., McNabb, R., Gudmundsson, G. H., Li, H. L., and Andreassen, L. M.: Results from ITMIX – the Ice Thickness Models Intercomparison eXperiment, in: EGU General Assembly Conference Abstracts, Vienna, Austria, 23-28 April, 2017, 4475, 2017.

Farinotti, D., Huss, M., Fürst, J. J., Landmann, J., Machguth, H., Maussion, F., and Pandit, A.: A consensus estimate for the ice thickness distribution of all glaciers on Earth, Nature Geoscience, 12, 168-173, https://doi.org/10.1038/s41561-019-0300-3, 2019.

Frey, H., Paul, F., and Strozzi, T.: Compilation of a glacier inventory for the western Himalayas from satellite data: methods, challenges and results, Remote Sensing of Environment, 124, 832-843, https://doi.org/10.1016/j.rse.2012.06.020, 2012.

Frey, H., Machguth, H., Huss, M., Huggel, C., Bajracharya, S., Bolch, T., Kulkarni, A., Linsbauer, A., Salzmann, N., and Stoffel, M.: Estimating the volume of glaciers in the Himalayan-Karakoram region using different methods, Cryosphere, 8, 2313-2333, https://doi.org/10.5194/tc-8-2313-2014, 2014.

Gao, H. K., Li, H., Duan, Z., Ren, Z., Meng, X. Y., and Pan, X. C.: Modelling glacier variation and its impact on water resource in the Urumqi Glacier No.1 in Central Asia, Science of the Total Environment, 644, 1160-1170, https://doi.org/10.1016/j.scitotenv.2018.07.004, 2018.

Gardelle, J., Berthier, E., Arnaud, Y., and Kääb, A.: Region-wide glacier mass balances over the Pamir-Karakoram-Himalaya during 1999-2011, Cryosphere, 7, 1263-1286, https://doi.org/10.5194/tc-7-1263-2013, 2013.

Gardner, A. S., Moholdt, Geir., Cogley, J. G., Wouters, B., Arendt, A. A., Wahr, J., Berthier, E., Hock, R., Pfeffer, W. T., Kaser, G., Ligtenberg, S. R. M., Bolch, T., Sharp, M. J., Hagen, J. O., van den Broeke, M. R., and Paul, F.: A reconciled estimate of glacier contributions to sea level rise: 2003 to 2009, Science (New York, N.Y.), 340, 1168, https://doi.org/10.1126/science.1234532, 2013.

Gärtner-Roer, I., Naegeli, K., Huss, M., Knecht, T., Machguth, H., and Zemp, M.: A dataset of worldwide glacier thickness observations, Global and Planetary Change, 122, 330-344, https://doi.org/10.1016/j.gloplacha.2014.09.003, 2014.

Grinsted, A.: An estimate of global glacier volume, The Cryosphere, 7, 141-151. https://doi.org/10.5194/tc-7-141-2013, 2013.

Guo, M. (Eds.): National Geographic of China, Huaxia Press, Beijing, 2011. [in Chinese]

Guo, W. Q., Liu, S. Y., Xu, J. L., Wu, L. Z., Shangguan, D. H., Yao, X. J., Wei, J. F., Bao, W. J., Yu, P. C., Liu,

https://doi.org/10.5194/essd-2020-71
Preprint. Discussion started: 7 September 2020

Open Access Earth System Science Data Discussions

Q., and Jiang, Z. L.: The second Chinese glacier inventory: data, methods and results, Journal of Glaciology, 61, 357-372, https://doi.org/10.3189/2015JoG14J209, 2015.

Guo, W. Q., Liu, S. Y., Yao, X. J., Xu, J. L., Shangguan, D. H., Wu, L. Z., Zhao, J. D., Liu, Q., Jiang, Z. L., Wei, J. F., Bao, W. J., Yu, P. C., Ding, L. F., Li, G., Li, P., Ge, C. M., and Wang, Y.: The Second Glacier Inventory Dataset of China (Version 1.0), Cold and Arid Regions Science Data Center at Lanzhou, https://doi.org/10.3972/glacier.001.2013.db, 2014.

Haeberli, W. and Hoelzle, M.: Application of inventory data for estimating characteristics of and regional climate-change effects on mountain glaciers: a pilot study with the European Alps, Ann. Glaciol., 21, 206-212, https://doi.org/10.1017/S0260305500015834, 1995.

Haeberli W., Bosch, H., Scherler, K., Østrem, G., and Wallen, C. C. (Eds.): World Glacier Monitoring Service (WGMS).: World Glacier Inventory – Status 1988, IAHS(ICSI)/UNEP/UNESCO, WGMS, Zurich, Switzerland, 458 pp., 1989.

Haeberli, W., Hoelzle, M., and Suter, S.: Into the Second Century of World-Wide Glacier Monitoring – Prospects and Strategies, Neuroence Letters, 158, 67-70, https://doi.org/10.1016/0304-3940(93)90614-Q, 1998.

Hajnsek, I., Krieger, G., Werner, M., Younis, M., and Zink, M.: TanDEM-X: a satellite formation for high-resolution SAR interferometry, IEEE Trans. Geosci. Remote Sens., 45, 3317-3341, https://doi.org/10.1109/TGRS.2007.900693, 2007.

Hiroko, B. and Rodell, M.: NASA/GSFC/HSL: GLDAS Catchment Land Surface Model L4 daily 0.25×0.25 degree V 2.0, Goddard Earth Sciences Data and Information Services Center (GES DISC), https://doi.org/10.5067/LYHA9088MFWQ, 2016.

Howat, I. M., Negrete, A., and Smith, B. E.: The Greenland Ice Mapping Project (GIMP) land classification and surface elevation data sets, Cryosphere, 8, 1509-1518, https://doi.org/10.5194/tcd-8-453-2014, 2014.

Huai, B. J., Li, Z. Q., Wang, F. T., Wang, W. B., Wang, P. Y., and Li, K. M.: Glacier volume estimation from ice-thickness data, applied to the Muz Taw glacier, Sawir Mountains, China, Environ. Earth Sci., 74, 1861-1870, https://doi.org/10.1007/s12665-015-4435-2, 2015.

Huang, M. H.: On the temperature distribution of glaciers in China, J. Glaciol., 36, 210-216, https://doi.org/10.1017/S002214300000945X, 1990.

Jiskoot, H. and Mueller, M. S.: Glacier fragmentation effects on surface energy balance and runoff: field measurements and distributed modelling, Hydrological Processes, 26, 1861-1875, https://doi.org/10.1002/hyp.9288, 2012.

Kääb, A., Nuth, C., Treichler, D., and Berthier, E.: Brief Communication: Contending estimates of early 21st century glacier mass balance over the Pamir-Karakoram-Himalaya, Cryosphere Discussions, 8, 5857-5874, https://doi.org/10.5194/tcd-8-5857-2014, 2014.

Kang, S. C., Xu, Y. W., You, Q. L., Flügel., W. A., Pepin, N., and Yao, T. D.: Review of climate and cryospheric change in the Tibetan Plateau, Environmental Research Letters, 5, 1748-1755, https://doi.org/10.1088/1748-9326/5/1/01501, 2010.

Kaushik, S., Joshi, P. K., and Singh, T.: Development of glacier mapping in Indian Himalaya: a review of approaches, International Journal of Remote Sensing, 40, 6607-6634, https://doi.org/10.1080/01431161.2019.1582114, 2019.

Klein, A. G., Kincaid, J. L., and Dobreva, I. D.: Improving glacier volume-area scaling to better quantify tropical

https://doi.org/10.5194/essd-2020-71
Preprint. Discussion started: 7 September 2020

Andean glacial water resources from remote sensing, in: AGU Fall Meeting Abstracts, San Francisco, 15-19 December, 2014, C31B-0290, 2014.

Lambrecht, A., Mayer, C., Hagg, W., Popovnin, V., Rezepkin, A., Lomidze, N., and Svanadze, D.: A comparison of glacier melt on debris-covered glaciers in the northern and southern Caucasus, The Cryosphere, 5, 525-538, https://doi.org/10.5194/tc-5-525-2011, 2011.

Lanzhou Institute of Glaciology and Geocryology (LIGG), Chinese academy of sciences. (Eds.): Glacier inventory of China (III): Altai Mountains, Science Press, Beijing, 1-206 pp., 1986. [in Chinese]

Li, B., Wei, Z., Li, X., He, Z., Zhang, K., and Wang, Z.: Records from Quaternary sediment and palaeo-environment in the Yangtze River Delta, Quaternary Sciences, 31, 316-328, https://doi.org/10.3969/j.issn.1001-7410.2011.02.14, 2011.

Li, J., Zheng, B., and Yang, X. (Eds.): The glaciers of Xizang (Tibet), Science Press, Beijing, 1986. [in Chinese]

Liu, J., Fang, J., Li, H. L., Cui, R. H., and Chen, M.: Dataset of GRACE gravity anomaly reconstruction in the Qinghai-Tibetan Plateau and adjacent areas (GRACEgravityTibet). Publishing system for scientific research data of global change, https://doi.org/10.3974/geodb.2016.06.07.V1, 2016.

Liu, J., Fang, J., Li, H. L., Cui, R. H., and Chen, M.: Secular variation of gravity anomalies within the Tibetan Plateau derived from GRACE data, Chinese Journal of Geophysics, 58, 3496-3506, https://doi.org/10.6038/cjg20151006, 2015.

Liu, S. Y., Sun, W. X., Shen, Y. P., and Li, G.: Glacier changes since the Little Ice Age maximum in the western Qilian Shan, northwest China, and consequences of glacier runoff for water supply, J. Glaciol., 49, 117-124, https://doi.org/10.3189/172756503781830926, 2003.

Liu, S. Y., Guo, W. Q., Yao, X., Xu, J., Shangguan, D., Wei, J., Liu, Q., Wang, X., and Jiang, Z.: Glacier change of China during the last 50 years as revealed by glacier inventories, in: AGU Fall Meeting Abstracts, San Francisco, 15-19 December, 2014, C43F-07, 2014.

Liu, Y. S., Qin, X., Chen, J. Z., Li, Z. L., Wang, J., Du, W. T., and Guo, W. Q.: Variations of Laohugou Glacier No.12 in the western Qilian Mountains, China, from 1957-2015, J. Mt. Sci., 15, 25-32, https://doi.org/10.1007/s11629-017-4492-y, 2018.

Liu, X. W.: Glacier volume dataset of the Qinghai-Tibetan Plateau in 1970s and 2000s, National Tibetan Plateau Data Center, 2020, https://doi.org/10.11888/Glacio.tpdc.270390, 2020.

Liu, Z. C., Wang, Y. J., Chen, Y., Li, X. S., and Li, Q. C.: Magnetostratigraphy and sedimentologically derived geochronology of the Quaternary lacustrine deposits of a 3000 m thick sequence in the central Qaidam basin, western China, Palaeogeography Palaeoclimatology Palaeoecology, 140, 0-473, https://doi.org/10.1016/S0031-0182(98)00048-0, 1998.

Liu, Z. X., Su, Z., Yao, T. D., Wang, W. T., and Shao, W. Z.: Resources and distribution of glaciers on the Tibetan Plateau, Resource Science, 2000, 22, 49-53, http://dx.doi.org/10.3321/j.issn:1007-7588.2000.05.011, 2000. [in Chinese]

Li, Z. G.: Glaciers and lakes changes on the Qinghai-Tibetan Plateau under climate change in the past 50 years, Journal of Natural Resources, 27, 1431-1443, https://doi.org/10.1007/s11783-011-0280-z, 2012.

Li, Z., Xing, Q., Liu, S. Y., Zhou, J. M., and Huang, L.: Monitoring thickness and volume changes of the Dongkemadi Ice Field on the Qinghai-Tibetan Plateau (1969-2000) using Shuttle Radar Topography Mission and map data, International Journal of Digital Earth, 5, 516-532, https://doi.org/10.1080/17538947.2011.594099, 2012.

Luo, T. X., Pan, Y. D., Ouyang, H., Shi, P. L., Ji, L., Yu, Z. L., and Lu, Q.: Leaf area index and net primary productivity along subtropical to alpine gradients in the Tibetan Plateau, Global Ecology & Biogeography, 13, 345-358, https://doi.org/10.1111/j.1466-822x.2004.00094.x, 2004.

Ma, L. L., Tian, L. D., and Pu, J. C.: Recent area and ice volume change of Kangwure Glacier in the middle of Himalayas, Chin. Sci. Bull., 55, 1766–1774, https://doi.org/10.1007/s11434-010-3211-7, 2010.

Ma, L. L., Tian, L. D., and Yang, W.: Measuring the depth of Gurenhekou Glacier in the South of the Tibetan Plateau using GPR and estimating its volume based on the outcomes, J. Glaciol. Geocryol., 30, 783–788, 2008. [in Chinese]

Mi, D., Xie, Z., Luo, X., Feng, Q., Ma, M., and Jin, D. (Eds.): Glacier inventory of China XI. The Ganga drainage basin, XII. The Indus drainage basin, Xi'an Cartographic Publishing House, Xi'an, China, 2002. [in Chinese]

Mool, P. K., Bajracharya, S. R., Shrestha, B., Joshi, S. P., Shakya, K., Baidya, A., and Dangol, G. S.: Inventory of Glaciers, Glacier Lakes and the Identification of Potential Glacial Lake Outburst Floods (GLOFs) Affected by Global Warming in the Mountains of Himalayan Region, International Centre for Integrated Mountain Development, Kathmandu, India, Open File Rep. 2004-03-CMY-Campbell, 48 pp., 2007.

Moor, E. J. and Stoffel, M.: Changing monsoon patterns, snow and glacial melt, its impacts and adaptation options in northern India: Synthesis. Science of the Total Environment, 468-469, S162-S167, https://doi.org/10.1016/j.scitotenv.2013.11.058, 2013.

Neckel, N., Kropáček, J., Bolch, T., and Hochschild, V.: Glacier mass changes on the Tibetan Plateau 2003-2009 derived from ICESat laser altimetry measurements, Environmental Research Letters, 9, https://doi.org/10.1088/1748-9326/9/1/014009, 2014.

Pu, J. (Eds): Glacier inventory of China IX. The Lancang river. X. The Nujiang river, Xi'an Cartographic Publishing House, Xi'an, 2001. [in Chinese]

Qiu, J.: The third pole, Nature, 454, 393-396, https://doi.org/10.1038/454393a, 2008.

Qi, W. W., Zhang, B. P., Pang, Y., Zhao, F., and Zhang, S.: TRMM-Data-Based Spatial and Seasonal Patterns of Precipitation in the Qinghai-Tibet Plateau, Scientia Geographica Sinica, 33, 999-1005, 2013. [in Chinese]

Rabus, B., Eineder, M., Roth, A., and Bamler, R.: The Shuttle radar topography mission: a new class of digital elevation models acquired by spaceborne radar, ISPRS J. Photogram. Remote Sens., 57, 241-262, https://doi.org/10.3390/s8053355, 2003.

Raup, B., Kieffer, H., Hare, T., and Kargel, J.: Generation of data acquisition requests for the ASTER satellite instrument for monitoring a globally distributed target: Glaciers, IEEE Transactions on Geoscience and Remote Sensing, 38, 1105-1112, https://doi.org/10.1109/36.841989, 2000.

Raup, B., Racoviteanu, A., Khalsa, S. J. S., Helm, C., Armstrong, R., and Arnaud, Y.: The GLIMS geospatial glacier database: A new tool for studying glacier change, Global and Planetary Change, 56, 0-110, https://doi.org/10.1016/j.gloplacha.2006.07.018, 2007.

RGI Consortium.: Randolph Glacier Inventory – A Dataset of Global Glacier Outlines: Version 4.0, Global Land Ice Measurements from Space, https://doi.org/10.7265/N5-RGI-40, 2014.

Shangguan, D., Liu, S. Y., Ding, Y. J., Zhang, Y. S., Li, J., Li, X. Y., and Wu, Z.: Changes in the elevation and extent of two glaciers along the Yanglonghe River, Qilian Shan, China, J. Glaciol., 56, 309-317, https://doi.org/10.3189/002214310791968566, 2010.

Shi, Y. and Li, J. (Eds.): Glaciological research of the Qinghai–Xizang Plateau in China, In Geological and

https://doi.org/10.5194/essd-2020-71
Preprint. Discussion started: 7 September 2020

ecological studies of Qinghai–Xizang Plateau. Vol. 2, Environment and ecology of Qinghai–Xizang Plateau, Science Press, Beijing, 1981. [in Chinese]

Shi, Y. F., Liu, C. H., and Kang, E. S.: The Glacier Inventory of China, Annuals of Glaciology, 50, 1-4, https://doi.org/10.3189/172756410790595831, 2009.

Shi, Y. F., Liu, S. Y., Ye, B., Liu, C., and Wang, Y. (Eds.): Concise glacier inventory of China, Shanghai Popular Science Press, Shanghai, China, 2008. [in Chinese]

Soller, D. R. and Garrity, C. P.: Map of bedrock topography, U.S. Geological Survey, Map 3392, 2018.

Sun, B., Wen, J. H., and He, M. B.: Measure the depth of the Arctic Ocean sea-ice using GPR and analyze its underside morphology, Sci. China (Series D), 32, 951–958, https://doi.org/10.3321/j.issn:1006-9267.2002.11.010, 2002.

Thompson, L. G., Mosley-Thompson, E., Davis, M. E., Bolzan, J. F., Dai, J., Klein, L., Gundestrup, N., Yao, T., Wu, X., and Xie Z.: Glacial stage ice-core records from the subtropical Dunde ice cap, China, Annuals of Glaciology, 14, 288-297, https://doi.org/10.1017/S0260305500008776, 1990.

Thompson, L. G., Mosley-Thompson, E., Davis, M. E., Bolzan, J. F., Dai, J., Yao, T., Gundestrup, N., Wu, X., Klein, L., and Xie, Z.: Holocene—Late Pleistocene climatic ice core records from Qinghai-Tibetan Plateau, Science, 246, 474-477, https://doi.org/10.1126/science.246.4929.474, 1989.

Thompson, L. G., Mosley-Thompson, E., Davis, M. E., Lin, P. N., Dai, J., Bolzan, J. F., and Yao, T. D.: A 1000 year climate ice-core record from the Guliya ice cap, China: its relationship to global climate variability, Annuals of Glaciology, 21, 175-181, https://doi.org/10.1017/S0260305500015780, 1995.

Vieli Leysinger, G. J.-M. C. and Gudmundsson, G. H.: A numerical study of glacier advance over deforming till, The Cryosphere, 4, 359-372, https://doi.org/10.5194/tc-4-359-2010, 2010.

Wang, G. X., Qian, J., Cheng, G. D., and Lai, Y. M.: Soil organic carbon pool of grassland soils on the Qinghai-Tibetan Plateau and its global implication, Science of the Total Environment, 291, 207-217, https://doi.org/10.1016/S0048-9697(01)01100-7, 2002.

Wang, N. L. and Pu, J. C.: Ice thickness, sounded by ground penetrating radar, on the Bayi Glacier in the Qilian Mountains, China, Journal of glaciology and Geocryology, 31, 431–435, 2009. [in Chinese]

Wang, P. Y., Li, Z. Q., Xu, C. H., Zhou, P., Wang, W. B., Jin, S., and Li, H. L.: Primary investigation of statistical correlation between changes in ice volume and area of glaciers, Sciences in Cold and Arid Regions, 11, 41-49, https://doi.org/10.3724/SP.J.1226.2019.00041, 2019.

Wei, J. F., Liu, S. Y., Xu, J. L., Guo, W. Q., Bao, W. J., Shangguan, D. H., and Jiang, Z. L.: Mass loss from glaciers in the Chinese Altai Mountains between 1959 and 2008 revealed based on historical maps, SRTM, and ASTER images, J. Mt. Sci., 12, 330-343, https://doi.org/10.1007/s11629-014-3175-1, 2015.

WGMS (World Glacier Monitoring Service).: Glacier Thickness Database 2.0, World Glacier Monitoring Service, Zurich, Switzerland, https://doi.org/10.5904/wgms-glathida-2016-07, 2016.

Wu, K. P., Liu, S. Y., Jiang, Z. L., Xu, J. L., and Wei, J. F.: Glacier mass balance over the central Nyainqentanglha Range during recent decades derived from remote-sensing data, Journal of Glaciology, 65, 422-439, https://doi.org/10.1017/jog.2019.20, 2019.

Wu, L. H., Li, Z. Q., and Wang, P. Y.: Sounding the Sigong River Glacier no. 4 in Mt. Bogda area the Tian shan Mountain by using ground penetrating Radar and estimating the ice volume, J. Glaciol. Geocryol., 33, 276–282, 2011. [in Chinese]

Wu, L. and Li, X. (Eds.): China glacier information system, Ocean Press, Beijing, 2004. [in Chinese]

https://doi.org/10.5194/essd-2020-71
Preprint. Discussion started: 7 September 2020

Xu, J., Liu, S., Zhang, S., Guo, W., and Wang, J.: Recent changes in glacial area and volume on Tuanjiefeng Peak region of Qilian Mountains, China, PLOS ONE, 8, e70575. https://doi.org/10.1371/journal.pone.0070574, 2013.

Yao, T. D., Thompson, L. G., Mosbrugger, V., Zhang, F., Ma, Y. M., Luo, T. X., Xu, B. Q., Yang, X. X., Joswiak, D. R., and Wang, W. C.: Third Pole Environment (TPE). Environmental Development, 3, 52-64, https://doi.org/10.1016/j.envdev.2012.04.002, 2012a.

Yao, T. D., Thompson, L. G., Yang, W., Yu, W. S., Cao, Y., Guo, X., J., Yang, X. X., Duan, K. Q., Zhao, H, B., Xu, B. Q., Pu, J. C., Lu, A. X., Xiang, Y., Kattel, D. B., and Joswiak, D.: Different glacier status with atmospheric circulations in Tibetan Plateau and surroundings, Nature Climate Change, https://doi.org/10.1038/NCLIMATE1580, 2012b.

Yao, Y. H. and Zhang, B. P.: The mass elevation effect of the Tibetan Plateau and its implications for Alpine treelines, International Journal of Climatology, 35, 1833-1846, https://doi.org/10.1002/joc.4123, 2015.

Zhang, G. Q., Yao, T. D., Xie, H. J., Wang, W. C., and Yang, W.: An inventory of glacier lakes in the Third Pole region and their changes in response to global warming, Global and Planetary Change, 131, 148-157, https://doi.org/10.1016/j.gloplacha.2015.05.013, 2015.

Zhang, Y. S., Liu, S. Y., Shangguan, D. H., Li, J., and Zhao, J. D.: Thinning and Shrinkage of Laohugou No.12 Glacier in the Western Qilian Mountains, China, from 1957 to 2007, J. Mt. Sci., 9, 343-350, https://doi.org/10.1007/s11629-009-2296-4, 2012.

Zhang, Z., Liu, S. Y., Wei, J. F., Xu, J. L., Guo, W. Q., Bao, W. J., and Jiang, Z. L.: Mass change of glaciers in Muztag Ata-Kongur Tagh, eastern Pamir, China from 1971/76 to 2013/14 as derived from remote sensing data, PLOS ONE, 11, e0147327, https://doi.org/10.1371/journal.pone.0147327, 2016.

Zhu, M. L., Yao, T. D., and Yang, W.: Ice volume and characteristics of sub glacial topography of the Zhadang Glacier, Nyaingntanglha Range, J. Glaciol. Geocryol., 36, 268–277, http://dx.doi.org/10.7522/j.issn.1000-0240.2014.0033, 2014. [in Chinese]

Zhu, M. L., Yao, T. D., Yang, W., Xu, B. Q., Wu, G. J., and Wang, X. J.: Differences in mass balance behavior for three glaciers from different climatic regions on the Tibetan Plateau, Clim. Dyn., 50, 3457-3484, https://doi.org/10.1007/s00382-017-3817-4, 2018.

Zwally, H. J., Jun, L. I., Brenner, A. C., Beckley, M., Cornejo, H. G., Dimarzio, J., Giovinetto, M. B., Neumann, T., Robbins, J. W., Saba, J. L., Yi, D. H., and Wang, W. L..: Greenland ice sheet mass balance: distribution of increased mass loss with climate warming, 2003-07 versus 1992-2002, J. Glaciol., 57, 88-102, https://doi.org/10.3189/002214311795306682, 2011.

https://doi.org/10.5194/essd-2020-71
Preprint. Discussion started: 7 September 2020

Appendix

Table A1 Observed glacier information in the QTP

Mountains	Glaciers	LON	LAT	S1 (km^2)	S2 (km^2)	L1 (m)	L2 (m)	Period	Reference
Qilian	Shule_1	97.71	38.60	13.236	12.330	7520	3305	1966-2006	
Qilian	Shule_2	97.86	38.51	10.427	9.824	6831	4135	1966-2006	
Qilian	Shule_3	98.69	38.23	15.619	16.79	6797	5505	1966-2007	
Qilian	Shule_4	97.79	38.46	15.054	14.95	7069	5932	1966-2006	Gärtner-Roer et al., 2014
Qilian	Shule_5	97.31	38.70	7.749	13.88	2462	4790	1966-2006	
Qilian	Shule_6	97.24	38.71	15.414	13.82	6795	6470	1966-2006	
Qilian	Shule_7	97.22	38.75	1.576	12.18	4555	2413	1966-2006	
Qilian	Bayi	98.57	39.23	6.675	4.076	4830	3748	1956-2007	Wang & Pu, 2009
Nyainqentanglha	Zhadang	90.67	30.47	1.92	1.68	2224	1451	2001-2009	Zhu et al., 2014
Nyainqentanglha	Gurenhekou	90.45	30.19	1.574	1.333	2834	2086	2001-2009	Ma et al., 2008

Note: S1, S2, L1, and L2 represent the glacier area in the RGI 4.0 and GIC-II and lengths of glaciers in the RGI 4.0 and GIC-II, respectively.